

Research Articles | Behavioral/Cognitive

Self-awareness from whole-body movements

<https://doi.org/10.1523/JNEUROSCI.0478-24.2024>

Received: 19 March 2024

Revised: 14 September 2024

Accepted: 19 October 2024

Copyright © 2024 the authors

This Early Release article has been peer reviewed and accepted, but has not been through the composition and copyediting processes. The final version may differ slightly in style or formatting and will contain links to any extended data.

Alerts: Sign up at www.jneurosci.org/alerts to receive customized email alerts when the fully formatted version of this article is published.

Self-awareness from whole-body movements

Authors: Akila Kadambi^{1*}, Gennady Erlikhman¹, Micah Johnson¹, Martin M. Monti^{1,2,3}, Marco Iacoboni², Hongjing Lu^{1,4}

Affiliations:

1. Department of Psychology, University of California Los Angeles, Los Angeles, CA, USA
2. Department of Psychiatry and Biobehavioral Sciences, David Geffen School of Medicine, University of California Los Angeles, Los Angeles, CA, USA
3. Department of Neurosurgery, Brain Research Center, David Geffen School of Medicine, University of California Los Angeles, Los Angeles, CA, USA
4. Department of Statistics, University of California Los Angeles, Los Angeles, CA, USA

* Corresponding author: akadambi@ucla.edu

Abstract (150 words)

Humans can recognize their whole-body movements even when displayed as dynamic dot patterns. The sparse depiction of whole-body movements, coupled with a lack of visual experience watching ourselves in the world, has long implicated non-visual mechanisms to self-action recognition. We aimed to identify the neural systems for this ability. Using general linear modeling and multivariate analyses on human brain imaging data from male and female participants, we first found that cortical areas linked to motor processes, including frontoparietal and primary somatomotor cortices, exhibit greater engagement and functional connectivity when recognizing self-generated versus other-generated actions. Next, we show that these regions encode self-identity based on motor familiarity, even after regressing out idiosyncratic visual cues using multiple regression representational similarity analysis. Last, we found the reverse pattern for unfamiliar individuals: encoding localized to occipito-temporal visual regions. These findings suggest that self-awareness from actions emerges from the interplay of motor and visual processes.

Significance Statement: We report for the first time that self-recognition from visual observation of our whole-body actions implicates brain regions associated with motor processes. On functional neuroimaging data, we found greater activity and unique representational patterns in brain areas and networks linked to motor processes when viewing our own actions relative to viewing the actions of others. These findings introduce an important role of motor mechanisms in distinguishing the self from others.

Introduction

41
42 Self-recognition is possible even from visually minimalistic dot-displays (Johansson,
43 1973; Cutting & Kozlowski, 1977; Loula et al., 2005). These displays, called point-light
44 displays (PLDs), depict whole-body actions with around a dozen moving dots (Johansson,
45 1973; Cutting & Kozlowski, 1977; Loula et al., 2005). While glimpses of our whole-bodies
46 may be captured in videos or glass mirrors, they are far less observable than the rich
47 visual experiences we have seeing movements of close friends or family members. Yet,
48 humans recognize their own movements better than familiar others' in PLDs (Loula et al.,
49 2005; Beardsworth & Buckner, 1981). This self-recognition advantage persists across
50 viewpoints (Jokisch et al., 2006; Prasad & Shiffrar, 2009), task judgments (Knoblich &
51 Flach, 2001; Bischoff et al., 2012), body parts (Frassinetti et al., 2009; Daprati & Sirigu,
52 2002), and action types (Burling et al., 2019; Kadambi et al., 2024), suggesting that self-
53 action recognition relies on modalities more than vision alone. Despite consistent
54 behavioral evidence, the neural mechanisms remain untested, representing a crucial gap
55 in understanding human self-awareness.

56 Neuroimaging studies in visual neuroscience often omit the self and focus on the
57 neural mechanisms coding other people's actions. These studies show that action
58 recognition engages a distributed network of cortical areas, termed action observation
59 network (AON). This network consists of occipito-temporal (OT) (posterior superior
60 temporal sulcus (pSTS), extrastriate body area, fusiform gyri) and frontoparietal circuits
61 engaged during action production, including inferior parietal lobe (IPL), premotor cortex
62 (PM), inferior frontal cortex (IFC), and supplementary motor area (SMA). The crucial
63 connection between OT and frontoparietal regions is via pSTS-IPL direct connections,
64 bridging action recognition via visual processing with cognitive theories of action
65 simulation (Ürgen et al., 2019; Grèzes et al., 2003).

66 While OT regions encode actions irrespective of identity, frontoparietal and
67 somatomotor regions may be critical for self-recognition. These regions are attributed
68 action simulation, or mirroring, functions— mapping observed actions onto one's own
69 motor system. For instance, spiking activity from single and multi-units recorded first in
70 frontoparietal regions in macaques (Di Pellegrino et al., 1992; Fogassi et al, 2005) and
71 later in medial frontal cortex (likely pre-SMA) in humans (Mukamel et al., 2010) during
72 action observation show similar activity during action production. This correspondence in
73 spiking activity is further seen with systems-level activity in these regions during brain
74 imaging and is modulated by the observer's motor familiarity with the action (Rizzolatti &
75 Craighero, 2004; Iacoboni, 2009; Calvo-Marino et al., 2006). Since self-generated actions
76 are most motorically familiar, this could be one mechanism to help differentiate self and
77 other actions.

78 To date, few neuroimaging studies have investigated self-action recognition from
79 PLDs. These studies support frontoparietal involvement, but used isolated body parts
80 (Bischoff et al., 2012; Macuga and Frey, 2011) or actions that were not self-generated,
81 but associated with self-identity (Woźniak et al., 2022). Hence, the neural mechanisms
82 supporting self-recognition of whole-body actions remain untested. Moreover, beyond
83 regional univariate activity, representational markers are needed to elucidate the featural
84 space supporting self-recognition. Using representational similarity analysis (RSA;
85 Kriegeskorte et al., 2008) can be a viable tool to localize and infer the type of information
86 encoded in neural activity patterns.

87 In the present study, we asked the following: which neural systems underlie self-
88 recognition from whole-body actions? Does self-action recognition rely more on motor
89 mechanisms, even after accounting for distinctive visual features of the actions, as compared to
90 other identities? To address these questions, we conducted a multimodal imaging study across
91 two sessions. In Session 1, we motion-captured a range of actions of participants and their close
92 friend of the same sex. These actions were performed using both visual instruction (imitation)
93 and verbal instruction (freely performed). After a delay period, participants returned in Session 2
94 for fMRI where they underwent an identity-recognition task on PLDs of themselves, friends, and
95 strangers.

96 We hypothesized that AON would be involved during action observation for all identities
97 (self, friends, strangers), encoded in occipito-temporal regions. However, we expected that
98 frontoparietal regions associated with motor processes would greater engage for the self,
99 controlling for visual familiarity (friend) and person identity (stranger). Moreover, if these regions
100 encode motor information to achieve self-recognition, then we expected that activity patterns in
101 frontoparietal and motor regions would relate to motor familiarity with actions, captured over and
102 above visual feature contributions.

103

104

Materials and Methods

105 Participants

106 Twenty right-handed undergraduate participants ($M_{age} = 20.55$, $SD_{age} = 1.73$, females = 12,
107 males = 8) were recruited from around the University of California, Los Angeles area using
108 convenience sampling. All participants were provided payment for their participation. Sample
109 size was based on prior fMRI studies most similar to ours using biological motion (e.g., Saygin
110 et al., 2004; Chang et al., 2021; Engelen et al., 2015) and self-generated point-light displays
111 (Bischoff et al., 2012). The study was approved by the UCLA Institutional Review Board. All
112 participants were naïve to the purpose of the study. Participants had normal or corrected-to-
113 normal vision and no physical disabilities.

114 Apparatus

115 The Microsoft Kinect V2.0 and Kinect SDK were used for motion-capture of actions, as in
116 previous studies on self-action recognition (Kadambi et al., 2024; Burling et al., 2019).
117 Customized software developed in our lab was used to enhance movement signals, and to carry
118 out additional processing and trimming for actions presented later in the testing phase (Van
119 Boxtel & Lu, 2013). Three-dimensional (X-Y-Z) coordinates of the key joints were extracted at a
120 rate of approximately 33 frames per second. Each action was trimmed to the start and stop of a
121 T-position signaled by the participant and normalized to scale for use in the experimental task.
122 Note that while motion capture accuracy was high, the Kinect occasionally produced noise
123 jittering in the stimuli, where frame-to-frame joints positions occasionally showed sudden jumps
124 in position. Hence, to remove noisy frame-to-frame jitter, we impinged a manual correction for
125 certain frames (i.e., replacing with the closest previous frame where the jitter was not present).

126 **Stimuli**

127 Twelve actions were selected from our previous work on self-action recognition (Burling et al.,
128 2019; Kadambi and Lu, 2019; Kadambi et al., 2024). These actions conveyed a range of
129 variability in terms of action planning. Six of the actions (i.e. *argue, wash windows, get attention,*
130 *hurry up, stretch, and play guitar*) were categorized as “verbally instructed actions”, delineated
131 by a high degree of motor goal complexity as defined in our previous work (Burling et al., 2019;
132 Kadambi et al., 2024). These actions were verbally instructed to the participant (e.g., please
133 perform the action: “to argue”). The remaining six actions were visually instructed (imitation)
134 actions, depicting a range of simple and complex goals (i.e., *jumping jacks, basketball, digging,*
135 *chopping, laughing, directing traffic*). For these actions, participants observed a stick figure
136 performing an action without any verbal label provided and were then instructed to ‘imitate the
137 movements of the action.’ These stick figure actions were selected from the Carnegie Mellon
138 Graphics (CMU) Lab Motion Capture Database available online (<http://mocap.cs.cmu.edu>),
139 generated from actors whose motions were already pre-captured. PLDs were thus created using
140 the above method for each participant, a sex-matched friend, and a sex-matched stranger. The
141 stranger's action was randomly selected from one of three possible distractors for each sex (six
142 total), pre-captured from actions of two of the experimenters and research assistants. The
143 categorization of the action types, in addition to providing variability of the action goal, allowed
144 us to further explore secondary analyses contrasting actions involving less motor familiarity due
145 to copying someone else’s motor plan (visual instruction) versus actions that involved more
146 motor familiarity due to freely performing the action (verbal instruction).

147

Procedure

148 *Behavioral Session*

149 In the first session, participants’ body movements were recorded using the Microsoft Kinect V2.0
150 and Kinect SDK in a quiet testing room. Participants were instructed to perform the actions in a

151 rectangular space, in order to provide flexibility in how to perform the action, while remaining
152 within recording distance. The Kinect was placed 1.5 m above the floor and 2.59 m away from
153 the participant. Participants were instructed to naturalistically perform 12 actions as described
154 above and recorded by our motion capture system. Participants signaled the start and stop of
155 action performance by performing an outstretched T-Pose with their arms. Participant actions
156 were then recorded and converted to point-light stimuli for use in the fMRI session.

157 Each of the 20 participants also brought a close friend of the same sex, who was also
158 separately recorded with the same paradigm. None of the participants were informed about the
159 study's purpose on self-recognition, but were informed that this study was about general visual
160 action processing. We used the recordings of the close friend in the fMRI session to assess the
161 impact of visual familiarity. After the recording session, participants completed a few attitudinal
162 questionnaires including the Autism-Spectrum Quotient (AQ; Baron-Cohen et al., 2001),
163 Schizotypal Personality Questionnaire (SPQ; Raine, 1991), and Vividness of Motor Imagery-2
164 (VMIQ-2; Roberts et al., 2008). These questionnaires were selected since they measure motor
165 simulation ability (VMIQ-2) or disturbances in sensorimotor self-recognition (SPQ, AQ).

166
167 **[Fig 1.tif]**
168

169
170 *fMRI session*

171 After a delay period of two to three weeks (mean delay days = 18.55, $SD = 2.87$), participants
172 returned for fMRI brain imaging in Session 2 (trial structure depicted in Figure 1). During brain
173 imaging, participants passively observed a point-light display consisting of 25 joints. These joints
174 included the head (head, neck, clavicle; 3 dots), arm (biceps, elbows, wrists; 6 dots), hands
175 (fingers; 6 dots), stomach (1 dot), hips (3 dots), knees (2 dots), leg (shin, feet; 4 dots). Each
176 point-light display either showed their own action (self), same-sex familiar friend, or same-sex

177 stranger action for a five second duration. The same-sex stranger was selected at random (out
178 of two options) between participants. After the stranger was selected, this stranger was
179 consistently used for all actions involved in the experiment for this participant. Following the five
180 second observation of the action, participants were prompted to identify on the next screen
181 whether the action video shown was their own, friend, or stranger within a two second maximum
182 response period. Participants responded with their right hand by pressing one of three keys,
183 having the index finger on the first, the middle finger on the second, and the ring finger on the
184 third key. One identity was assigned to each key, and identity-key mapping was
185 counterbalanced across subjects. Participants' response was followed by jittered intertrial
186 intervals (ITI) mean-centered at 5 seconds. There were four runs per participant, each
187 consisting of 36 trials (12 trials per identity condition) in an event-related design. For each run,
188 experimental conditions were pseudorandomized to reduce stimulus autocorrelation related to
189 order and sequence effects as well as correlated noise, such as scanner drift. Response
190 mapping of self/friend/stranger was randomized between participants to reduce effects of trial
191 structure or motor preparation and planning demands. Duration of the experimental task during
192 functional brain imaging was around 24 minutes. Total brain imaging duration lasted
193 approximately 45 minutes.

194

195 **Experimental Design and Statistical Analysis**

196

MRI Acquisition

197 The Siemens 3-Tesla Prisma Fit scanner at the Staglin IMHRO Center for Cognitive
198 Neuroscience was used for Magnetic resonance imaging, equipped with a 32-channel head coil.
199 Structural data was acquired using a T1-weighted MPRAGE protocol (1.0 mm³ resolution;
200 repetition time = 2000 ms). Functional data was acquired utilizing T2*-weighted Gradient Recall
201 Echo sequence. Scanning parameters for the main task included: repetition time = 700 ms, echo

202 time = 33 ms, voxel size = 2.5 mm³ voxels, field of view = 192 mm, flip angle = 70°. Four dummy
203 scans were acquired and discarded before each scan to account for scanner stabilization.
204 Participants viewed the stimuli presented on a projector through a mirror mounted on the head
205 cover in the scanner. Participants underwent four runs of 36 trials each. Each run lasted
206 approximately 360 seconds.

207 **Imaging Analyses**

208 **Univariate Analysis**

209 Statistical analyses were conducted using FEAT (fMRI Expert Analysis Tool) Version 6.00, part
210 of FSL (FMRIB's Software Library, www.fmrib.ox.ac.uk/fsl) using the GLM approach. Individual
211 functional scans were coregistered to the high resolution structural image using boundary-based
212 registration (Greve and Fischl, 2009). Registration of the high-resolution structural scan to the
213 Montreal Neurological Institute (MNI) template was implemented using FSL's FLIRT (Jenkinson
214 2001, 2002) with 12 parameter DOF affine transformation. The following pre-processing steps
215 were applied: motion correction using MCFLIRT (Jenkinson 2002); slice-timing correction using
216 Fourier-space time-series phase-shifting; non-brain tissue removal using BET (Smith 2002);
217 spatial smoothing using a Gaussian kernel of FWHM 5mm; grand-mean scaling of the entire 4D
218 dataset by a single multiplicative factor; high-pass temporal filtering (Gaussian-weighted
219 leastsquares straight line fitting, with sigma=50.0s). Regressors were defined based on the
220 onsets and durations of the three identities (self, friend, stranger) across all actions. Individual
221 runs were aggregated into a mixed effects higher-level model using FLAME (FMRIB's Local
222 Analysis of Mixed Effects) stage 1 and stage 2 (Beckmann et al., 2003; Woolrich, 2004;
223 Woolrich 2008) for both within-session single subject variance and between-session group level
224 variance. Significance testing on the statistical parametric maps was then assessed at the group
225 level using two approaches in FSL: (1) *randomise* with threshold-free cluster enhancement
226 (TFCE) and $p < .05$ FWE-corrected (Winkler et al., 2014; Smith & Nichols, 2009), TFCE- p

227 threshold = .05 and (2) random-field (RFT) based thresholding at $Z > 3.1$, cluster corrected to a
228 significance level of $p < .05$ (Worsley 2001). *Randomise* served as our main approach to
229 significance testing given its more conservative, specific, and sensitive significance criteria
230 (Smith & Nichols, 2009). All figures and tables generated from the parametric RFT analysis are
231 reported in Extended Data 5-2, 5-4, 5-5. Conjunction analysis to localize self-specific activity
232 was also implemented in FSL using the `easythresh_conj` script ([easythresh_conj](#)) on univariate
233 activation maps for both *self > stranger* and *self > friend* contrasts (Nichols et al., 2005; Price &
234 Friston, 1997). The conjunction specifically tested the “conjunction null hypothesis” as to
235 whether both conditions showed significant functional activation ($Z > 3.1$, $p < .05$), which were
236 later used as seed regions in the connectivity analyses.

237 *Functional connectivity: Psychophysiological Interaction (PPI)*

238 To identify a neural circuitry prioritized for self-processing, we implemented PPI (Friston et al.,
239 1997) to assess task-specific changes in functional connectivity. PPI examines how the
240 relationships between a seed region and voxels in other brain regions are modulated by the
241 psychological state of the participant (task-dependent). The degree to which the seed regions
242 and sink (other brain regions) vary as a function of the task, is measured by testing the
243 significance of the β coefficient of the interaction computed between the experimental contrast
244 vector and the sink region. As our analyses focused on identifying a self-action circuitry, we
245 constrained our seeds to those determined by group-level functional activations in separate
246 GLMs for the self (i.e., *self > stranger* or *self > friend* contrasts). We used a conjunction analysis
247 implemented in FSL using the `easythresh_conj` script ([easythresh_conj](#)) on univariate activation
248 maps for both *self > stranger* and *self > friend* contrasts. The seed region in the left IPL was
249 generated from creating a sphere (8mm radius) around the peak functional activation for the
250 conjunction of the *self > stranger* and *self > friend* contrasts (centered at peak center-of-gravity,
251 $x, y, z = -56, -44, 42$). We initially focused on the IPL in the left hemisphere, since the TFCE

252 thresholding only produced left hemispheric activity in the IPL. However, to more
253 comprehensively investigate IPL involvement during self-processing, we also conducted PPI
254 with the right hemisphere IPL seed. The seed regions were each defined in standard space and
255 resampled to match 2.5mm isotropic voxel resolution. The resampled masks were then inversely
256 transformed to native space, applied with nearest neighbor interpolation. Time courses in the
257 seed region were extracted using fslmeants (<https://fsl.fmrib.ox.ac.uk/fsl/fslwiki/Fslutils>), which
258 generated a vector of mean activity in the mask for each volume. This time course was then
259 entered as the ROI time series regressor into the PPI GLM. Thus, the full GLM consisted of the
260 interaction vector (PPI regressor), the main effects of the contrasts of interest (the psychological
261 variables), and a vector representing the seed region time course (the physiological variable, Y
262 regressor). At the group level, statistical parametric maps for the interaction term were
263 thresholded ($Z > 2.3$, $p < .01$) to compute significance of the interaction term.

264 **Representational Similarity Analysis**

265 Whole-brain representational dissimilarity analysis (RDA) (Haxby et al., 2014; Krieskegorte et
266 al., 2008) was implemented using the CoSMoMvPA toolbox (<http://www.cosmomvpa.org/>;
267 [Oosterhof et al., 2016](#)) and custom MATLAB scripts (R2020a). Regressors were defined based
268 on the onsets and durations of the three experimental conditions (self-actions, friend-actions, or
269 stranger-actions) during the action observation period of the task. Using the Least-Squares
270 Separate approach, beta-series parameter estimates (Rissman, Gazzaley, & D'Esposito, 2004;
271 Mumford et al., 2012) were iteratively estimated per trial by modeling a regressor for the event of
272 interest in the trial and a regressor for all other events within the run. Standard motion
273 parameters were also included as regressors in each GLM. Preprocessing was identical to the
274 univariate analysis, but no smoothing was applied. We generated multiple target
275 representational dissimilarity matrices (RDM)s based on differences related to spatiotemporal
276 movement distinctiveness (dynamic time warping), speed, acceleration, jerk, body structure

277 consisting of limb segment length, and a theoretical RDM based on proprioceptive familiarity. To
278 generate neural RDMs for each participant, we extracted 36 beta weights for each run,
279 normalized each beta weight within run, computed the average for each of the 36 action targets
280 across all runs, and then demeaned the data (i.e., subtraction of the grand mean of all averaged
281 targets from each averaged target). All RDMs (behavioral, theoretical, and neural) were square,
282 symmetric, and reflected the pairwise dissimilarity between each element in the matrix. Each
283 RDM (proprioceptive familiarity, identity, movement distinctiveness, speed, acceleration, jerk,
284 body structure) was either correlated separately with neural activity (standard RDA) or entered
285 as input into a multiple regression RDA with other RDMs. The RDMs in the multiple regression
286 analysis included a subset of the prior RDMs: proprioceptive familiarity and identity (self, friend,
287 or stranger), and visual feature-based models related to movement distinctiveness (DTW), and
288 speed. Each RDM was z-transformed prior to estimating the regression coefficients in the
289 multiple regression analysis.

290 For the whole-brain searchlight RDA, each searchlight window was defined by a
291 Gaussian sphere of 2-mm radius. Each spherical searchlight included every voxel in the brain,
292 along with neighboring voxels within the window. The standard searchlight RDA was
293 implemented through correlating the target RDM with neural RDM in each searchlight across the
294 whole-brain. The correlations were then Fisher-z transformed and mapped to the center of each
295 searchlight to create individual similarity maps in native space as inputs to the higher-level
296 nonparametric analyses. For the multiple regression searchlight RDA, a multiple regression
297 analysis was conducted in each searchlight across the whole-brain. For each participant in
298 native space, the betas were mapped to the center of each searchlight to create individual
299 similarity maps for each predictor as inputs to the higher-level non-parametric analyses. All
300 individual maps were normalized to the MNI-152 template using FSL's FLIRT functionality
301 (<https://fsl.fmrib.ox.ac.uk/fsl/fslwiki/FLIRT>) using trilinear interpolation for group-analysis. One-
302 sample t-tests were computed at the group level, correcting for multiple comparisons using

303 permutation-based threshold-free cluster enhancement with a corrected threshold of $p < 0.01$
304 (Smith and Nichols, 2009) with 10,000 Monte Carlo Simulations.

305
306
307

308
309
310
311
312

[Fig 2.tif]

313

Target Representational Dissimilarity Matrices:

314 Shown in Figure 2, we constructed the following representational dissimilarity matrices used as
315 predictors for both standard and multiple regression representational dissimilarity analyses:

316 **Movement Distinctiveness.** The behavioral RDM for movement distinctiveness was generated
317 using the dynamic time warping (DTW) algorithm to compare trajectory differences between a
318 pair of actions. DTW measures the pairwise movement dissimilarity between action time series
319 via an alignment procedure that accounts for variability in time series length or duration. DTW
320 aims to find the lowest cost function (warping path) between pairwise action time series that
321 stretches or shrinks the time series to reflect warped distances. Greater DTW values indicate
322 greater movement dissimilarity between joint trajectories. A 36 x 36 RDM was created for each
323 participant that computed the pairwise DTW dissimilarity between each of the 12 actions across
324 each identity (self, friend, stranger). The following steps were implemented for Dynamic Time
325 Warping (DTW) analysis in MATLAB R2020a:

326 (1) For each participant's actions, 3D positions of each of the 25 joints were extracted using
327 the BioMotion toolbox (van Boxtel & Lu, 2013).

328 (2) Each joint trajectory was centered to zero in order to remove the impact of global factors
329 (e.g., global body displacements, limb length, etc.) on the similarity measures.

- 330 (3) The action DTW algorithm (Pham, Le, & Le, 2014) was implemented to search for a
331 temporal warping function shared across all 25 joints.
- 332 (4) After deriving the optimal warping function, the analysis computed the frame-by-frame
333 Euclidean distances of the temporally warped joint trajectories in actions performed by
334 different actors.
- 335 (5) DTW distance was computed as the sum of the distances between all joint trajectories
336 normalized by the number of frames of a target actor. This normalization step is required
337 to account for the different durations across participants performing the same action.
- 338 (6) For each participant, the dissimilarity of the target participant performing an action from
339 all other identities was captured by a mean DTW distance measure, computed by
340 averaging across pairwise DTW distances between the target participant with the other
341 actors (friend, stranger) in performing this action to construct the 36 x 36
342 representational dissimilarity matrix (RDM).

343 **Speed, Acceleration, and Jerk Differences.** To measure the contribution of movement speed
344 to self-recognition, we calculated a speed distinctiveness value for every participant's individual
345 action in MATLAB R2020a. For each action, we computed the average 3D positional
346 displacement across all frames and all 25 joints (using the first-order derivative of position)
347 extracted from Biomotion Toolbox (Van Boxtel & Lu, 2013). We then computed the average
348 pairwise Euclidean distance to all other identities and actions as a measure of speed
349 distinctiveness to construct the 36 x 36 RDM. Acceleration and jerk were identically computed,
350 though taking the first and second derivative of speed respectively.

351 **Body Structure (postural limb length).** The body structure RDA was computed based on the
352 limb length of each of the 24 limbs (for 25 joints) of the PLD. Limb length was computed using
353 the 3D Euclidean distance between pairs of joints that made up each limb in the PLD. Pairwise

354 absolute value dissimilarities were then calculated across participants for each limb and
355 averaged together across all limbs to comprise the 36 x 36 target RDM.

356 **Motor familiarity.** We computed a simple theoretical RDM based on the theorized motor
357 familiarity between each of the identities. This was based on common coding theory (Prinz,
358 1997), which posits a common representational platform and shared overlap between visual and
359 motor codes. Thus, identity for the self was coded as 0 (most familiarity due to prior motor
360 experience; least dissimilarity). We coded friend as 0.6 to capture the low-medium level of
361 familiarity, since participants had a high degree of visual familiarity with the friends' actions,
362 translating to a small degree of motor familiarity. Note that the specific value of 0.6 was not
363 critical, as the main findings (as described in the results section) remained for a range of
364 possible values. Since common coding theory posits shared or overlapping visual and motor
365 codes, repeated visual exposure to friends' actions could establish partial motor simulation,
366 where repeated observation of common movements of familiar friends activates motor circuits
367 even without direct execution of those actions (Rizzolatti and Craighero, 2004; Gallese 2006).
368 This would account for stronger neural encoding seen for friends' actions compared to
369 strangers. Hence, stranger was coded as 1 for all actions (no familiarity; most dissimilarity).
370 Within self-identity, we further weighted the actions by their motor familiarity. Specifically,
371 actions that were more motorically familiar to participants due to freely performing the action and
372 self-generating the motor plan (i.e., via verbal instruction) were coded as most similar (0).
373 Actions that involved copying someone else's motor plan (i.e., imitated via visual instruction)
374 were coded as less familiar (.3). All other identities (friend, stranger) were computed equally
375 similar across actions (friend coded as 0.6, stranger coded as 1). Thus, dissimilarity was
376 computed between identities and weighted by motor familiarity to comprise the 36 x 36
377 theoretical RDM.

378 **Identity: Self (motor familiarity), Friend (visual familiarity), or Stranger.** We also computed
379 theoretical RDMs specific to identity for either self actions, friend actions, or stranger actions.
380 For each identity RDM, the identity of interest (e.g., self) was coded as 0 (most similar), while
381 the other two identities (e.g., friend, stranger) were coded equally as dissimilar (1). Dissimilarity
382 was only computed between identities (and not individual actions) to comprise 36 x 36
383 theoretical RDMs for each identity (self RDM, friend RDM, or stranger RDM).

384 Results

385 Identity recognition from sparse actions

386 First, we examined whether self-recognition was possible in visually sparse point-light displays.
387 We found that participants could discriminate all identities (self, friend, stranger) significantly
388 above chance (.33), self: $M = .563$, $SD = .180$, $t(19) = 5.789$, $p < .001$, cohen's $d = 1.29$; friend:
389 $M = .483$, $SD = .182$, $t(19) = 3.754$, $p = .001$, $d = .839$; stranger: $M = .5052$, $SD = .172$, $t(19) =$
390 4.554 , $p < .001$, $d = 1.01$ (Figure 3).

391
392
393
394 [Fig 3.tif]
395
396
397
398

399
400 Recognition of self-generated actions ($M = .563$, $SD = .180$) was significantly higher than
401 friends' actions ($M = .483$, $SD = .182$), $t(19) = 2.673$, $p_{\text{adj}} = .049$, $d = .598$, but not significantly
402 higher than correctly identifying strangers' actions ($M = .505$, $SD = .172$), $t(19) = 1.353$, $p_{\text{adj}} =$

403 .192. Self-recognition accuracy was also modulated by motor planning, revealed by a significant
404 interaction effect between action type and identity $F(2,19) = 7.546$, $p = .002$, $\eta_p^2 = .284$.
405 Specifically, actions that were generated by one's own motor plan (i.e., verbally instructed; $M =$
406 $.615$, $SD = .198$) were better recognized relative to actions that were performed by copying
407 someone else's motor plan (visually instructed, $M = .513$, $SD = .189$), $t(19) = 3.170$, $p_{adj} = .049$,
408 $d = .709$. This behavioral result supports the hypothesis that motor processes are involved in
409 self-recognition. Motor planning did not modulate recognition accuracy for any of the other
410 identities, friends $t(19) = .340$, $p = .999$, nor strangers, $t(19) = -2.195$, $p = .285$. All post-hoc
411 comparisons were corrected using Tukey's HSD.

412 As shown in the top panel of Figure 3, self-recognition was greatest for the stretch action
413 ($M = .788$, $SD = .412$) and lowest for digging ($M = .375$, $SD = .487$). Across all actions, no
414 relationships were found between self-recognition accuracy and distinctiveness related to speed
415 ($p = .747$), acceleration ($p = .380$), postural length ($p = .410$), or movement dissimilarity ($p =$
416 $.174$). These results confirm that action identity could be distinguished in the sparse visual
417 displays, with an advantage for actions generated with one's own motor plan.

418

419 **Action Observation Network is recruited for identity recognition**

420 Our main goal was to examine the neural mechanisms underlying self-recognition from whole-
421 body movements. To do so, we first compared neural activity for each identity (*self*, *friend*,
422 *stranger*) relative to baseline. We found bilateral recruitment of the action observation network
423 for all identities (overlaid in MNI space *Fig 4*). The activity spanned regions classically found in
424 visual neuroscience, including the posterior superior temporal sulcus (pSTS) (right: $x,y,z = 56,$
425 $42, 10$, left: $x,y,z = -52, -50, 10$) and lateral occipital cortices, including extrastriate body area
426 (EBA) (right $x,y,z = 44, -60, 10$; left $x,y,z = -51, -69, 10$),⁺ as well as regions with motor properties
427 also described in the action observation literature (Rizzolatti & Craighero, 2004; Bonini et al.,

428 2022), including the bilateral supplementary motor areas (right $x,y,z = 12, 6, 56$; left $x,y,z = 4, -8,$
429 52), premotor cortices (right $x,y,z = 39,1,53$; Left $x, y, z = -45, 2, 50$), inferior frontal gyri (IFG)
430 (right $x,y,z = 50, 15, 10$; left $x,y,z = -55, 16, 10$), and inferior parietal lobules (IPL) (right $x,y,z =$
431 $50, -40, 14$; left $x,y,z = -56, -44, 11$).

432
433
434
435
436
437
438
439
440

[Fig 4.tif]

A frontoparietal network for self-action processing

441 Though visual and motor systems were involved during action observation of all identities, we
442 expected greater activity in motor regions when participants observed their own actions, since
443 self-generated actions are privileged by prior motor experience. According to common coding
444 theory, vision and proprioception share a degree of functional equivalence, such that action
445 recognition is facilitated by a matching process between these modalities (Prinz 1997; Hommel
446 et al., 2001).

447 Since visual and proprioceptive codes are most closely matched when observing our
448 own actions relative to observing actions of others, self-recognition should be facilitated in brain
449 regions with motor properties that are also active during action observation (e.g., Knoblich and
450 Flach, 2004; Limanowski and Blankenburg, 2016; Abdulkarim et al., 2023). Indeed, both self
451 contrasts of interest (*self > stranger* and *self > friend*) uniquely evoked greater activity in
452 frontoparietal regions with these properties. For *self > stranger*, activity was localized to the left
453 posterior supramarginal gyrus (peak $x, y, z = -62, -48, 28$) into the angular gyrus, as well as the
454 left insular cortex and the inferior frontal gyrus, pars opercularis ($x,y,z = -42, 10, -8$) (Figure 5). A
455 few small clusters in the anterior cingulate cortex (ACC) ($x,y,z = -2, 20, 18$; $x,y,z = 4, 14, 28$) and

456 one small cluster in the right insular cortex ($x,y,z = 40, 10, -2$) were also observed. *Self > friend*
457 similarly recruited the left posterior SMG of the IPL ($x,y,z = -54, -50, 30$), spanning the angular
458 gyrus (Figure 5, right panel). For *friend > stranger* and *stranger > friend*, FSL's *randomise*
459 approach did not yield significant activity. All peak clusters from the analyses are reported in the
460 Extended Data Tables 5-1, 5-2, and 5-3.

461
462 [Figure 5.tif]
463

464
465
466 Coactivation in these regions does not necessarily implicate a network for self-processing. Thus,
467 we further measured network-related activity during self-processing using task-based functional
468 connectivity (PPI; Friston et al., 1997). The bilateral IPL (peak sphere from the group-level
469 conjunction maps for self-processing: left: $x, y, z = -56, -44, 42$; right: $54, -38, 40$) was set as
470 seed regions in separate PPIs, due to the important role of the IPL in motor simulation and hub
471 status in action processing.

472 We found very similar results across both hemispheric seeds. For both seed regions, we
473 observed strengthened frontoparietal and parieto-visual connectivity for the self-processing
474 contrasts (*self > stranger* and *self > friend*). The left IPL seed for *self > stranger* showed the
475 greatest peak connectivity between parieto-visual regions: the right lateral occipital cortex ($x, y,$
476 $z = 54, -50, -2$), and the left occipito-temporal fusiform area ($x, y, z = -52, -70, -12$). We also
477 found strengthened frontoparietal connectivity, specifically with the bilateral inferior frontal
478 cortices (left $x, y, z = -54, 16, 30$; right $x, y, z = 46, 18, 20$), as well as bilateral intraparietal
479 sulcus spanning the somatomotor cortex (left $x, y, z = 26, -50, 44$, right $x, y, z = 32, -36, 44$)
480 (Figure 6). For the right IPL seed, we found similar connectivity patterns to the left. For *self >*
481 *friend* with the right IPL seed, we found the greatest frontoparietal functional connectivity,
482 between the right IPL and the bilateral inferior frontal cortex ($x,y,z = -36, 30, 34$), extending from

483 the middle frontal gyrus to the IFG pars opercularis, and spanning the primary motor cortex and
484 premotor cortex. Additional activity was found in the right pre-SMA ($x,y,z = 4,12,58$) as well as
485 bilateral occipitotemporal regions, with peaks in the right occipital-temporal cortex ($x,y,z = 46, -$
486 $56, -2$) and left superior temporal sulcus ($x,y,z = -62, -50, 8$). For *self > stranger*, we observed
487 strengthened parieto-occipitotemporal activity, with peaks in the left lateral occipito-temporal
488 cortex ($x,y,z = -46, -68, 12$), and right fusiform area ($x,y,z = 42, -40, -20$). Additionally, we found
489 strengthened connectivity with the frontal lobe, with peaks in the bilateral inferior frontal cortex,
490 spanning the premotor and primary motor regions. No activity was found for *friend > stranger*.
491 All activity maps were cluster corrected at $Z > 2.3, p < .01$.

492

493

[Figure 6.tif]

494

495

496

497

498

499

500

501

502

503

504

505

506

507

508

509

510
 511
 512
 513
 514
 515
 516 **Table 1.** PPI results with bilateral IPL seeds

Region	Contrast	Hemisphere	Area	MNI (x,y,z)	Max Z	Cluster Size	p
Left IPL							
	Self > Stranger	Right	Fusiform Area	54, -50, -2	4.09	2265	<.0001
		Left	Fusiform Area	-52, -70, -12	4.09	1660	<.0001
		Right	IFC	46, 18, 20	4.05	1537	<.0001
		Left	IFC	-54, 16, 30	4.01	1932	<.0001
			IPS	32, -36, 44	3.56	807	<.0001
			IPS	-26, -50, 44	3.74	1142	<.0001
	Self > Friend	Right	IFC	50, 14, 44	3.83	629	<.0001
		Left	IFC	-50, 26, 28	3.69	1216	<.0001
		Right	Fusiform Area	42, -60, -10	3.93	1154	<.0001
		Left	Fusiform Area	-48, -50, -20	3.57	401	.003
		Left	Middle Temporal	-60, -50, 4	4.02	609	<.0001
Right IPL							
	Self > Stranger	Left	LOC	-46, -68, 12	3.91	1418	<.0001
		Right	Fusiform Area	42, -40, -20	3.57	1248	<.0001
		Right	IFC	38, 30, 20	3.58	885	<.0001
		Left	IFC	-44, 12, 28	3.63	703	<.0001

Left	STS	-62, -50, 8	3.57	781	<.0001
Right	Pre-SMA	4, 12, 48	3.78	576	<.0001
Right	OTC	46, -56, -2	3.32	482	.00031
Left	MFG	-36, 30, 34	3.43	415	.00111

517

518

Evaluating a visuomotor representational space for self-processing

519

Based on the strengthened frontoparietal connectivity for self-processing, the analysis below

520

focused on underlying representational structure. Specifically, we examined the extent to which

521

self-recognition relied on factors that resembled motor familiarity, while accounting for visual

522

signatures of the actions across the whole-brain using multiple regression RDA. We opted for

523

whole-brain analyses since frontoparietal regions often comprise multiple brain networks (e.g.,

524

action observation network, central executive network), and since additional regions associated

525

with motor functions also encode self-processing. If self-recognition relies on motor

526

mechanisms, then encoding patterns may further span other regions associated with motor

527

properties, such as the somatomotor cortex. Thereafter, we conducted four multiple regression

528

RDAs for the following predictors of interest: (1) motor familiarity and (2) for each identity: (2a)

529

self, (2b) friend, or (2c) stranger in separate regression models, accounting for visual features

530

related to speed or movement distinctiveness.

531

Multiple Regression Motor Familiarity RDA: somatomotor cortex and occipitotemporal regions

532

The motor familiarity representational dissimilarity matrix was computed based on the theorized

533

motor familiarity between each of the identities (self as most motorically familiar, friend as

534

medium, and stranger as least). Within self-identity, we further weighted the actions by their

535

degree of motor familiarity. Actions that were most motorically familiar to participants due to self-

536

generating the motor plan were coded as most similar. Actions that involved copying someone

537

else's motor plan (i.e., imitated via visual instruction) were coded as less familiar.

538 Shown in Figure 7, we found robust encoding in the somatomotor, frontoparietal, and
539 lateral-occipital cortices. Specifically, the motor familiarity multiple regression RDA (accounting
540 for differences in speed and movement distinctiveness) revealed the largest pattern of encoding
541 in the bilateral primary motor cortex (M1), spanning the primary somatosensory cortex (S1), and
542 showed stronger representation in the left hemisphere (left peak $x,y,z = -46, -22, 50$) than right
543 (right peak $x,y,z = 52, 1, 34$). Activity patterns were also found in fronto-parietal regions,
544 including inferior parietal (right peak $x,y,z: 54, -36, 36$, left peak $x,y,z: 46, -66, 34$), and a large
545 cluster spanning the anterior cingulate, mid-superior frontal areas, and supplementary motor
546 areas (right peak $x,y,z = 11, 50, 17$; left peak $x,y,z = -18, 3, 41$). Activity patterns were also
547 observed in the occipital and lateral-occipital regions, extending into the bilateral lingual gyrus,
548 precuneus, cuneus (right peak $x,y,z = 22, -61, -2$). These results together reveal a gradation of
549 encoding in motor-related regions using identity-based motor familiarity. Specifically, motor-
550 related brain regions were most strongly encoded when viewing self-generated actions, followed
551 by friend, and followed by stranger. An exhaustive table of all activity patterns is reported in
552 Extended Data Table 7-1.

553

554

555

[Fig 7.tif]

556

557

558 *Multiple Regression Identity RDAs: stronger representation in somatomotor cortex and mPFC*

559 We then measured whether the representational encoding found in these regions was

560 specialized for self-identity. We compared activity patterns generated from multiple regression

561 RDAs that specified self-actions as the predictor of interest, as compared to multiple regression
562 RDAs for each other identity (friend, or stranger).

563 The self-identity RDA generated the largest activity patterns in the bilateral somatomotor
564 regions, with its peak in the left hemisphere (left peak $x,y,z = -30,-23,57$) and visually identified
565 in the right hemisphere (right peak $x,y,z = 40, -12, 50$) (Figure 8). We also found large activity
566 patterns in frontoparietal regions, spanning the IPL (left peak $x,y,z = -37,-64,40$; right peak x,y,z
567 $= 60,-36,27$), supplementary motor area (left peak $x,y,z = -8,-7,58$, right peak $x,y,z = 11,15,58$),
568 and lateral to medial-prefrontal cortices (peak $x,y,z = 46,50,4$) for the self-identity multiple
569 regression RDA. These results suggest that the somatomotor and frontoparietal regions—
570 associated with motor simulation—primarily encoded self-actions relative to actions of others.
571 Further, the strength of encoding in the somatomotor and frontoparietal cortices systematically
572 degraded as a function of identity. Specifically, the friend RDA produced less encoding, and the
573 stranger RDA produced no significant encoding in these regions. Activity patterns were also
574 most visually distributed for the self, followed by friend, and followed by stranger (examined at a
575 reduced threshold, $p < .05$).

576 Additional activity patterns unique to self-identity were also found in bilateral
577 parahippocampal gyri (left peak $x,y,z = -16,-13,-20$, right peak $x,y,z = 32,-28,-4$), with much
578 smaller activity patterns found in the left occipital pole (left peak $x,y,z = -23,-98,-14$), bilateral
579 temporal pole (right peak $x,y,z = 46,4,-33$, left peak $x,y,z = -32,-39,16$), thalamus (peak $x,y,z =$
580 $14,-22,18$), and precuneus (peak $x,y,z = 8,-38,6$). For the friend RDA, the activity patterns were
581 noticeably sparser and largely overlapped with self-identity, but mostly constrained to the
582 cortical midline. These regions spanned the precentral gyri, SMA, IPL, insula (peak $x,y,z = -46,-$
583 $30, 23$), the left calcarine and occipitotemporal regions (peak $x,y,z = -16, -61, 16$), and thalamus
584 (peak $x,y,z = -8, 34, -0$). For the stranger RDA, only sparse activity patterns were found in visual
585 regions: right middle temporal gyrus and occipitotemporal cortex (peak $x,y,z = 62, -47, 6$) at a

586 reduced threshold ($Z > 1.96$). See Extended Data (Tables 8-1, 8-2, 8-3) for an exhaustive report
587 of all clusters from all RDAs, visually depicted in Figure 8.

588
589
590
591
592
593
594

[Fig 8.tif]

Table 2. Number of voxels in regions of interest for each main identity RDA. Table depicts a parametric degradation in activity pattern encoding in somatomotor and frontoparietal regions as a function of person-identity.

Area	Self	Friend	Stranger
Somatomotor	5675	1843	0
Frontoparietal			
IPL	2383	913	2
SPL	1192	481	0
IFG	860	322	0
INS	740	198	0

595
596 *Abbreviations:* IPL (Inferior Parietal Lobule); SPL (Superior Parietal Lobule); IFG (Inferior Frontal Gyrus);
597 IS (Insular Cortex). Number of voxels calculated within region of interest (ROI) masks generated from
598 Harvard-Oxford Cortical Atlas for each identity RDA map (self, friend: $p_s < 0.01$, and stranger: $p < 0.05$).
599 Somatomotor mask was generated by combining precentral and postcentral gyri masks. IPL mask
600 determined by the combination of parietal operculum, angular gyri, and supramarginal gyri (anterior and
601 posterior) masks, subtracting occipito-temporal overlap (medial temporal gyri and lateral occipital cortices).
602 IFG mask determined by combination of IFG pars triangularis and IFG pars opercularis masks. Insula
603 mask determined by subtracting IFG mask from Insula ROI.
604

605 Finally, to account for any effect of motor planning of the button responses producing the
606 large motor cluster in the left-hemisphere for the self-RDA, we conducted an additional RDA for
607 self-identity that included the timing of the motor responses as a covariate in the multiple
608 regression analysis. The results maintained the original findings of the self-RDA. Specifically,
609 the largest cluster from the RDA was observed in the left somatomotor cortex (left peak $x,y,z =$
610 $42, -20, 46$), and preserved the main findings. See Extended Data (Table 9-1) for an exhaustive
611 report of all clusters from the RDA, visually depicted in Figure 9.

612

613

[Figure 9.tif]

614

615 Combined with results from the motor familiarity RDA, these findings lend support to
616 motor simulation accounts. Self-processing, due to its high degree of motor familiarity, would be
617 expected to have the strongest degree of motor simulation during action observation, reflected
618 by the largest activity patterns in motor-related regions, followed by friend, then stranger. This
619 aligns with prevalent accounts suggesting that action observation of others involves an internal
620 simulation of the action onto our own motor systems (e.g., Rizzolatti & Craighero, 2004;
621 Iacoboni, 2008).

622

623 Discussion

624 Our study investigated the neural correlates for self-recognition of our whole-body movements.
625 On functional brain imaging data, we report that merely observing our whole bodies in motion
626 evokes greater activity in neural systems traditionally construed as having motor functions, in
627 comparison to observing the actions of others.

628 While boundaries between visual and motor functions have been increasingly blurred
629 over the last few decades of systems neuroscience research, traditionally frontoparietal areas
630 are mostly conceived as having motor functions, whereas occipito-temporal areas are typically
631 construed as involved in visual processing. Here, we found that both areas were involved in
632 action observation of all identities. However, unique to self-action observation, we observed
633 greater activity and functional connectivity of frontoparietal regions (left inferior parietal lobule;
634 IPL and inferior frontal cortex; IFC), functionally connected to occipito-temporal regions. Note
635 that significance for all univariate subtraction contrasts was assessed using non-parametric
636 threshold-free cluster enhancement (TFCE), as TFCE has been shown to be more sensitive yet
637 less prone to false positives in the literature (Smith & Nichols, 2009). This resulted in left-
638 lateralized activity for self-processing. However, bilateral involvement of these regions was
639 clearly observed when using FSL's standard RFT cluster correction ($Z > 3.1$, $p < .05$) as well as

640 in our multivariate analyses. To avoid false positives, we interpret the non-parametric results,
641 but do not make strong claims on observed laterality.

642 Action simulation accounts posit a central role of the motor system during action
643 observation (Gallese & Goldman, 1998; Rizzolatti & Sinigaglia, 2010). The degree of motor
644 experience with actions is thought to parametrically modulate activity in these frontoparietal and
645 motor regions during action observation (even across modalities, e.g., Kaplan et al., 2008;
646 Kirsch and Cross, 2015; Blakemore & Frith, 2003). Since self-generated actions benefit from
647 prior motor experience, action simulation could be one candidate mechanism for the increased
648 activity and connectivity in these regions. However, these regions, notably frontoparietal, also
649 support functions beyond action simulation, including working memory (Baddeley, 2003),
650 cognitive control (Corbetta & Shulman, 2002), and multisensory integration (Macaluso & Driver,
651 2005). While we are unaware of any direct links between cognitive control and self-recognition
652 on a visual perception task—multisensory integration, particularly in the IPL, could be an
653 important mechanism to facilitate self-action recognition by combining visual and proprioceptive
654 information. Similarly, working memory could facilitate retention of the action in order to
655 differentiate identity, implicating the intraparietal sulcus and numerous occipitotemporal regions
656 (Woźniak et al., 2022).

657 It is important to note that merely observing actions may not veridically engage the same
658 cognitive and neural resources associated with action simulation. For instance, while action
659 observation can engage sensorimotor areas, it may not trigger the same internal model
660 mechanisms that would predict somatosensory attenuation during action production, as
661 expected in action simulation accounts (Kilteni et al., 2021). Conversely, other processes such
662 as motor imagery, can engage these mechanisms (Kilteni et al., 2018). Hence, we do not make
663 strong claims on positing the functional mechanism associated with these areas, but highlight
664 action simulation as one possible candidate.

665 Strengthened connectivity was also observed between the bilateral IPL and the inferior
666 frontal cortex (IFC) anterior to the premotor cortex, during self-action recognition. Action
667 simulation accounts often implicate both the IFC and IPL, two anatomically and functionally
668 connected areas. Other proposals suggest that anterior parcellations of the IFC might be locally
669 involved in abstracted aspects of action understanding, such as goal selection, intention
670 inference, and semantic understanding (e.g., Liakakis et al., 2011). During self-action
671 recognition, the IFC (including its more anterior portions) could support the integration of action
672 observation with higher-order cognitive processes. Information flow may originate from
673 strengthened parieto-occipitotemporal functional connectivity during action processing, then
674 passed onto the IFC (in both anterior and posterior IFG in our data) for more conceptual action
675 understanding.

676 Our results also highlight the role of parieto-occipitotemporal regions in action
677 observation. These regions may distinguish fine-grained visual features that facilitate
678 discrimination between identities. Together with the IPL and the IFC (e.g., Kilner, 2011), this set
679 of areas may form an expanded action observation network for self-recognition. That is,
680 occipital-temporal regions first decode coarse visual identity based on low and mid-level action
681 features (including for person perception in the superior temporal sulcus, Isik et al., 2017), while
682 frontoparietal regions may process self-actions at a deeper motoric, proprioceptive, and
683 conceptual level (e.g., Rizzolatti et al., 2014; Rizzolatti & Craighero, 2004).

684 In addition to frontoparietal and occipitotemporal regions engaged during self-action
685 observation, the multivariate results revealed largest activity patterns in bilateral somatomotor
686 regions. Activity in these regions for both the motor familiarity and self-identity representational
687 (dis)similarity analyses (RSA)s spanned the primary motor, primary somatosensory,
688 supplementary motor areas, and the premotor cortices. Further, the strength of encoding in the
689 somatomotor and frontoparietal cortices systematically degraded as a function of identity. These

690 regions most strongly encoded self-identity, moderately encoded friend-identity, and did not
691 encode stranger-identity, which instead revealed activity patterns in primarily occipito-temporal
692 regions. The relatively parametric degradation of somatomotor and frontoparietal encoding as a
693 function of person identity lends further support to action simulation accounts.

694 While neural activity in these frontoparietal and somatomotor regions is often implicated
695 in motor production (e.g., Muir and Lemon, 1983) as well as control, attention, and working
696 memory processes as noted earlier, these regions are often functionally implicated in tasks
697 involving action simulation, including action observation (Gallese & Goldman, 1998; Keysers
698 and Gazzola, 2010), motor imagery (Schnitzler et al., 1997; Ehrsson et al., 2003; Porro et al.,
699 2000; Pilgramm et al., 2016; Pfurtscheller & Neuper, 1997), action prediction (Lamm, Fischer &
700 Decety, 2007; Blakemore and Frith, 2003), motor memory (Romo et al., 2012), and motor
701 planning (Gale et al., 2021). Moreover, coactivation in both premotor and posterior parietal
702 areas appears to depend on the match between motor and visual information that facilitates
703 one's sense of body ownership (e.g., Abdulkarim et al., 2023). The greater match between
704 common visual and proprioceptive codes may provide the increased sense of bodily awareness
705 needed to facilitate self-recognition. This is reflected by the greater signal encoding in these
706 regions for the self, which degraded by visuomotor person familiarity (i.e., less for friend, none
707 for stranger).

708 The RSA results also revealed that the neural encoding was most distributed for self-
709 identity, followed by friend, and least for stranger, where it was primarily localized to occipito-
710 temporal regions. A substantial body of research suggests that self-processing generally
711 engages systems-wide and distributed activity compared to processing other identities (e.g.,
712 Molnar-Szakacs & Uddin, 2013; Turk et al., 2003; Yeshurun et al., 2021). Indeed, at the
713 network-level, self-processing involves strong interactions between both low-level feature-based

714 processing, and higher-level conceptual processing, facilitating a sense of identity due to the
715 wealth of information we have stored about our own identities (Molnar-Szakacs & Uddin, 2013).

716 Results from the self-identity RSA also revealed distributed encoding patterns in other
717 regions (see Extended Data Table 8-1). The activity patterns spanned regions traditionally
718 associated with mentalizing (Frith & Frith, 2006) and higher-order reflective and conceptual self-
719 and other-processing, including the bilateral posterior cingulate cortex, medial (and lateral)
720 prefrontal cortex, bilateral hippocampus, and the precuneus. These regions not only engage
721 during mentalizing for others, but also for conceptual mentalizing about oneself (Lombardo et
722 al., 2010; Qin and Northoff, 2011), and conscious awareness of oneself (e.g., Tacikowski et al.,
723 2017). Well-known action frameworks (e.g., Keysers and Gazzola, 2007) characterize a degree
724 of dynamic connectivity between simulative motor representations and abstracted, self-reflective
725 judgments. It is possible that these regions may store action representations in memory, or
726 motor schemas, which are later accessed as a comparison to the visual consequence during
727 action observation (Schmidt, 1975; Arbib 1981; Arbib, 1992). That is, rather than identifying
728 one's body based solely on visual cues that we generally lack access to in daily life, we may
729 access stored proprioceptive schemas at a more abstract level of processing (i.e., "remembered
730 selves"; Neisser, 1988) that interact with action observation to facilitate the visuo-proprioceptive
731 match needed for self-recognition.

732 Finally, a cluster of activity in the anterior cingulate cortex (ACC) was also observed in
733 the RSA as well as a small cluster during the univariate task contrast of *self* > *stranger* actions.
734 While ACC engagement may be due to multiple reasons given the many functional processes it
735 has been associated with, a key account of ACC function is related to cognitive conflict (Braver
736 et al., 2001). Prior research has shown that the ACC is involved in discriminating one's own
737 touch from an external touch, with the activity linked to the conflict between expected and actual
738 sensorimotor feedback (Blakemore et al 1998; Kiltner et al 2024; Stetson et al 2006). There may
739 be a similar conflict mechanism here when participants merely view their own and other people's

740 actions. The brain has well-established representations of self-generated actions, and viewing
741 these actions might generate conflict between the internal sensorimotor expectations and the
742 stimulus-driven visual feedback during action observation. This conflict should be less
743 pronounced, or even absent when viewing others' actions, since the internal sensorimotor
744 predictions for others' actions are less accessible.

745 In summary, our three main analyses— univariate, functional connectivity, and RSA—
746 converge on a cortical ensemble of visuomotor regions, spanning frontoparietal, somatomotor,
747 and occipito-temporal areas, that seem prioritized for self-recognition of whole-body actions.
748 These regions, notably frontoparietal and somatomotor cortices, are often linked to simulative
749 motor functions during action observation, which may provide a functional explanation for the
750 increased motor-related activity we observed. Our findings together reveal an important
751 contribution of motoric indices to human self-awareness, helping to facilitate the basic
752 differentiation between ourselves and others.

753 **Acknowledgements**

754 We thank Sophia Baia and Kelly Xue for assistance with data collection and stimuli creation, and
755 Elinor Yeo, Jolie Wu, Kelly Nola, Nicolas Jeong, Danya Elghebagy, David Lipkin, Shahan
756 McGahee for assistance with stimuli creation. We thank Jeff Chiang, Burcu Ürgen, and
757 Giuseppe Marrazzo for helpful advice on the analyses. We thank Lisa Aziz-Zadeh and Sofronia
758 Ringold for helpful feedback on an earlier draft of this manuscript. This project was supported by
759 National Science Foundation BCS- 2142269 to H.L., UCLA faculty research grant to H.L., Tiny
760 Blue Dot Foundation grant to M.M.M., and APA Dissertation Award to A.K. Preliminary versions
761 of this project were presented at the Virtual Society for Neuroscience (2020), V-Vision Sciences
762 Society (2020), Society for Neuroscience (2022), and Association for Scientific Study of
763 Consciousness (2023).

764

765 **Data Availability:** All analysis scripts, behavioral data, and results from the imaging analyses
766 can be downloaded from our GitHub repository: <https://github.com/akilakada/self-fmri>. Raw nifti
767 data can be shared upon request to the corresponding author and subject to the UCLA
768 Institutional Review Board Guidelines.

769

770

771
772
773
774
775
776
777
778
779
780
781
782
783
784
785
786
787
788
789
790
791
792
793
794
795
796
797
798
799
800
801
802
803
804
805
806
807
808
809
810
811
812
813
814
815

References

- Abdulkarim, Z., Guterstam, A., Hayatou, Z., & Ehrsson, H. H. (2023). Neural substrates of body ownership and agency during voluntary movement. *Journal of Neuroscience*, 43(13), 2362-2380.
- Apps, Matthew AJ, and Manos Tsakiris. "The free-energy self: a predictive coding account of self-recognition." *Neuroscience & Biobehavioral Reviews* 41 (2014): 85-97.
- Arbib, M. A. (1981). Perceptual structures and distributed motor control. In *Handbook of physiology, section I: the nervous system, vol. 2: motor control* (ed. V. B. Brooks), pp. 1449–80. Williams and Wilkins, Baltimore
- Arbib, M. A. (1992). Schema theory. *The encyclopedia of artificial intelligence*, 2, 1427-1443.
- Aron AR, Fletcher PC, Bullmore ET, Sahakian BJ, Robbins TW (2003) Stop-signal inhibition disrupted by damage to right inferior frontal gyrus in humans. *Nat Neurosci* 6:115–116.
- Asakage, S., & Nakano, T. (2023). The salience network is activated during self-recognition from both first-person and third-person perspectives. *Human Brain Mapping*, 44(2), 559-570.
- Astafiev, S. V., Stanley, C. M., Shulman, G. L., & Corbetta, M. (2004). Extrastriate body area in human occipital cortex responds to the performance of motor actions. *Nature neuroscience*, 7(5), 542-548.
- Atkinson, A. P., Dittrich, W. H., Gemmell, A. J., & Young, A. W. (2004). Emotion perception from dynamic and static body expressions in point-light and full-light displays. *Perception*, 33(6), 717-746.
- Baddeley, A. (2003). Working memory: looking back and looking forward. *Nature Reviews Neuroscience*, 4(10), 829-839.
- Baron-Cohen, S., Wheelwright, S., Skinner, R., Martin, J., & Clubley, E. (2001). The autism spectrum quotient (AQ): evidence from Asperger syndrome/high-functioning autism, males and females, scientists and mathematicians. [erratum appears in *J Autism Dev Disord* 2001 Dec;31(6):603]. *Journal of Autism & Developmental Disorders*.
- Beckmann, C. F., Jenkinson, M., & Smith, S. M. (2003). General multilevel linear modeling for group analysis in fMRI. *Neuroimage*, 20(2), 1052-1063.
- Beardsworth, T., & Buckner, T. (1981). The ability to recognize oneself from a video recording of one's movements without seeing one's body. *Bulletin of the Psychonomic Society*, 18(1), 19-22.
- Benjamini, Y., & Yekutieli, D. (2001). The control of the false discovery rate in multiple testing under dependency. *Annals of statistics*, 1165-1188.

816 Berlucchi, G., & Aglioti, S. M. (2010). The body in the brain revisited. *Experimental brain*
817 *research*, 200(1), 25-35.

818

819 Blakemore, S. J., & Frith, C. (2003). Disorders of self-monitoring and the symptoms of
820 schizophrenia. *The self in neuroscience and psychiatry*, 407-424.

821

822 Blakemore, S. J., Frith, C. D., & Wolpert, D. M. (1999). Spatio-temporal prediction modulates the
823 perception of self-produced stimuli. *Journal of cognitive neuroscience*, 11(5), 551-559.

824

825 Blakemore SJ, Wolpert DM, Frith CD. Central cancellation of self-produced tickle sensation. *Nat*
826 *Neurosci*. 1998 Nov;1(7):635-40. doi: 10.1038/2870. PMID: 10196573.

827

828 Blanke, O. (2012). Multisensory brain mechanisms of bodily self-consciousness. *Nature*
829 *Reviews Neuroscience*, 13(8), 556-571.

830

831 Blanke, O., Slater, M., & Serino, A. (2015). Behavioral, neural, and computational principles of
832 bodily self-consciousness. *Neuron*, 88(1), 145-166.

833

834 Bischoff, M., Zentgraf, K., Lorey, B., Pilgramm, S., Balsler, N., Baumgartner, E., ... & Munzert, J.
835 (2012). Motor familiarity: Brain activation when watching kinematic displays of one's own
836 movements. *Neuropsychologia*, 50(8), 2085-2092.

837

838 Bracci S, Caramazza A, Peelen MV (2015) Representational similarity of body parts in human
839 occipitotemporal cortex. *J Neurosci* 35:
840 12977–12985. CrossRef Medline

841

842 Braver, T. S., Barch, D. M., Gray, J. R., Molfese, D. L., & Snyder, A. (2001). Anterior cingulate
843 cortex and response conflict: effects of frequency, inhibition and errors. *Cerebral cortex*, 11(9),
844 825-836.

845

846 Bréchet, L., Grivaz, P., Gauthier, B., & Blanke, O. (2018). Common recruitment of angular gyrus
847 in episodic autobiographical memory and bodily self-consciousness. *Frontiers in behavioral*
848 *neuroscience*, 270.

849

850 Brady N, Campbell M, Flaherty M (2004) My left brain and me: a dissociation in the perception
851 of self and others. *Neuropsychologia* 42:1156–1161.

852

853 Burling, J. M., Kadambi, A., Safari, T., & Lu, H. (2019). The impact of autistic traits on
854 selfrecognition of body movements. *Frontiers in psychology*, 9, 2687.

855

856 Calvo-Merino, B., Grèzes, J., Glaser, D. E., Passingham, R. E., & Haggard, P. (2006). Seeing or
857 doing? Influence of visual and motor familiarity in action observation. *Current biology*, 16(19),
858 1905-1910.

859

860 Candidi, M., Stienen, B. M., Aglioti, S. M., & de Gelder, B. (2011). Event-related repetitive
861 transcranial magnetic stimulation of posterior superior temporal sulcus improves the detection of
862 threatening postural changes in human bodies. *Journal of Neuroscience*, 31(48), 17547-17554.
863

864 Chang, D. H., Troje, N. F., Ikegaya, Y., Fujita, I., & Ban, H. (2021). Spatiotemporal dynamics of
865 responses to biological motion in the human brain. *Cortex*, 136, 124-139.s
866

867 Cisler, J. M., Bush, K., & Steele, J. S. (2014). A comparison of statistical methods for detecting
868 context-modulated functional connectivity in fMRI. *Neuroimage*, 84, 1042-1052.
869

870 Conson, M., Aromino, A. R., & Trojano, L. (2010). Whose hand is this? Handedness and visual
871 perspective modulate self/other discrimination. *Experimental Brain Research*, 206(4), 449-453.
872

873 Corbetta, M., & Shulman, G. L. (2002). Control of goal-directed and stimulus-driven attention in
874 the brain. *Nature Reviews Neuroscience*, 3(3), 201-215.
875

876 Coste, A., Bardy, B. G., Janaqi, S., Słowiński, P., Tsaneva-Atanasova, K., Goupil, J. L., & Marin,
877 L. (2021). Decoding identity from motion: how motor similarities colour our perception of self and
878 others. *Psychological research*, 85(2), 509-519.
879

880 David, N., Cohen, M. X., Newen, A., Bewernick, B. H., Shah, N. J., Fink, G. R., et al. (2007). The
881 extrastriate cortex distinguishes between the consequences of one's own and others'
882 behavior. *Neuroimage*, 36, 1004e1014.
883

884 Darda, K. M., & Ramsey, R. (2019). The inhibition of automatic imitation: A meta-analysis and
885 synthesis of fMRI studies. *NeuroImage*, 197, 320-329.
886

887 De Bellis, F., Trojano, L., Errico, D., Grossi, D., & Conson, M. (2017). Whose hand is this?
888 Differential responses of right and left extrastriate body areas to visual images of self and others'
889 hands. *Cognitive, Affective, & Behavioral Neuroscience*, 17(4), 826-837.
890

891 de Gelder B (2006) Towards the neurobiology of emotional body language. *Nat Rev Neurosci*
892 7:242–249.
893

894 de Gelder B (2009) Why bodies? Twelve reasons for including bodily expressions in affective
895 neuroscience. *Philos Trans R Soc Lond B Biol Sci* 364:3475–3484.
896

897 Desmurget, M., Epstein, C. M., Turner, R. S., Prablanc, C., Alexander, G. E., & Grafton, S. T.
898 (1999). Role of the posterior parietal cortex in updating reaching movements to a visual target.
899 *Nature neuroscience*, 2(6), 563-567.
900

901 Devue, C., Collette, F., Balteau, E., Degueldre, C., Luxen, A., Maquet, P., & Brédart, S. (2007).
902 Here I am: the cortical correlates of visual self-recognition. *Brain research*, 1143, 169-182.
903

904 Di Pellegrino, G., Fadiga, L., Fogassi, L., Gallese, V., & Rizzolatti, G. (1992). Understanding
905 motor events: a neurophysiological study. *Experimental brain research*, 91(1), 176-180.
906

907 Downing, P. E., Jiang, Y., Shuman, M., & Kanwisher, N. (2001). A cortical area selective for
908 visual processing of the human body. *Science*, 293(5539), 2470e2473. [http://dx.doi.org/10.1126/](http://dx.doi.org/10.1126/science.1063414)
909 [science.1063414](http://dx.doi.org/10.1126/science.1063414).
910

911 Downing, P. E., Peelen, M. V., Wiggett, A. J., & Tew, B. D. (2006). The role of the extrastriate
912 body area in action perception. *Social Neuroscience*, 1(1), 52-62.
913

914 Downing, P. E., Chan, A. Y., Peelen, M. V., Dodds, C. M., & Kanwisher, N. (2006). Domain
915 specificity in visual cortex. *Cerebral cortex*, 16(10), 1453-1461.
916

917 Ehrsson, H. H., Geyer, S., & Naito, E. (2003). Imagery of voluntary movement of fingers, toes,
918 and tongue activates corresponding body-part-specific motor representations. *Journal of*
919 *neurophysiology*.
920

921 Engelen, T., de Graaf, T. A., Sack, A. T., & de Gelder, B. (2015). A causal role for inferior
922 parietal lobule in emotion body perception. *cortex*, 73(195), e202.
923

924 Fogassi, L., Ferrari, P. F., Gesierich, B., Rozzi, S., Chersi, F., & Rizzolatti, G. (2005). Parietal
925 lobe: from action organization to intention understanding. *Science*, 308(5722), 662-667.
926

927 Friston, K. J., Buechel, C., Fink, G. R., Morris, J., Rolls, E., & Dolan, R. J. (1997).
928 Psychophysiological and modulatory interactions in neuroimaging. *Neuroimage*, 6(3), 218-229.
929

930 Gallese, V., & Goldman, A. (1998). Mirror neurons and the simulation theory of mind-reading.
931 *Trends in cognitive sciences*, 2(12), 493-501.
932

933 Gallese, V. (2006, October). Embodied simulation: from mirror neuron systems to interpersonal
934 relations. In *Empathy and Fairness: Novartis Foundation Symposium 278* (pp. 3-19). Chichester,
935 UK: John Wiley & Sons, Ltd.
936

937 Genovese, C. R., Lazar, N. A., & Nichols, T. (2002). Thresholding of statistical maps in
938 functional neuroimaging using the false discovery rate. *Neuroimage*, 15(4), 870-878.
939

940 Goldenberg, G., & Spatt, J. (2009). The neural basis of tool use. *Brain*, 132(6), 1645-1655.
941

942 Graziano, M. S., Taylor, C. S., & Moore, T. (2002). Complex movements evoked by
943 microstimulation of precentral cortex. *Neuron*, 34(5), 841-851.
944

945 Graziano, M. S. (2016). Ethological action maps: a paradigm shift for the motor cortex. *Trends in*
946 *cognitive sciences*, 20(2), 121-132.
947

948 Greve, D. N., & Fischl, B. (2009). Accurate and robust brain image alignment using boundary-
949 based registration. *Neuroimage*, 48(1), 63-72.
950
951 Grèzes J, Armony JL, Rowe J, Passingham RE. Activations related to “mirror” and “canonical”
952 neurones in the human brain: an fMRI study, *Neuroimage.*, 2003, vol. 18 (pg. 928-937)
953
954 Haaland, K. Y., Harrington, D. L., & Knight, R. T. (2000). Neural representations of skilled
955 movement. *Brain*, 123(11), 2306-2313.
956
957 Haaland, K. Y. (2006). Left hemisphere dominance for movement. *The clinical*
958 *neuropsychologist*, 20(4), 609-622.
959
960 Haxby, J. V., Connolly, A. C., & Guntupalli, J. S. (2014). Decoding neural representational
961 spaces using multivariate pattern analysis. *Annual review of neuroscience*, 37, 435-456.
962
963 Hodzic, A., Kaas, A., Muckli, L., Stirn, A., & Singer, W. (2009). Distinct cortical networks for the
964 detection and identification of human body. *Neuroimage*, 45(4), 1264-1271.
965
966 Hohmann, T., Troje, N. F., Olmos, A., & Munzert, J. (2011). The influence of motor expertise
967 and motor experience on action and actor recognition. *Journal of Cognitive Psychology*, 23(4),
968 403– 415. Return to ref 2011 in article
969
970 Iacoboni, M., Koski, L. M., Brass, M., Bekkering, H., Woods, R. P., Dubeau, M. C., ... &
971 Rizzolatti, G. (2001). Reafferent copies of imitated actions in the right superior temporal cortex.
972 *Proceedings of the national academy of sciences*, 98(24), 13995-13999.
973
974 Iacoboni, M., Molnar-Szakacs, I., Gallese, V., Buccino, G., Mazziotta, J. C., & Rizzolatti, G.
975 (2005). Grasping the intentions of others with one's own mirror neuron system. *PLoS biology*,
976 3(3), e79.
977
978 Iacoboni, M. (2008). *Mirroring people: The new science of how we connect with others*. Farrar,
979 Straus and Giroux.
980
981 Iacoboni, M. (2009). Imitation, empathy, and mirror neurons. *Annual review of psychology*, 60,
982 653-670.
983
984 Ionta S, Heydrich L, Lenggenhager B, Mouthon M, Fornari E, Chapuis D, Gassert R, Blanke O.
985 Multisensory mechanisms in temporo-parietal cortex support self-location and first-person
986 perspective. *Neuron*. 2011 Apr 28;70(2):363-74. doi: 10.1016/j.neuron.2011.03.009. PMID:
987 21521620.
988
989 Isik, L., Koldewyn, K., Beeler, D., & Kanwisher, N. (2017). Perceiving social interactions in the
990 posterior superior temporal sulcus. *Proceedings of the National Academy of Sciences*, 114(43),
991 E9145-E9152.
992

993 Jackson, P. L., & Decety, J. (2004). Motor cognition: A new paradigm to study self–other
994 interactions. *Current opinion in Neurobiology*, 14(2), 259-263.
995
996 Jeannerod, M. Visual and action cues contribute to the self–other distinction. *Nat Neurosci* 7,
997 422– 423 (2004). <https://doi.org/10.1038/nn0504-422>
998 Jeannerod, M., & Pacherie, E. (2004). Agency, simulation and self-identification. *Mind &*
999 *language*, 19(2), 113-146.
1000
1001 Jenkinson, M and Smith, S. A global optimisation method for robust affine registration of brain
1002 images. *Medical Image Analysis*, 5(2):143-156, 2001.
1003
1004 Jenkinson, M., Bannister, P., Brady, J., and Smith, S. Improved optimisation for the robust and
1005 accurate linear registration and motion correction of brain images. *NeuroImage*, 17(2):825-841,
1006 2002.
1007
1008 Johansson, G. (1973). Visual perception of biological motion and a model for its analysis.
1009 *Perception & psychophysics*, 14, 201-211.
1010
1011 Jokisch, D., Daum, I., & Troje, N. F. (2006). Self recognition versus recognition of others by
1012 biological motion: Viewpoint-dependent effects. *Perception*, 35(7), 911-920.
1013
1014 Kadambi A, Xie Q, Lu H (2024) Individual differences and motor planning influence self-
1015 recognition of actions. *PLoS ONE* 19(7): e0303820.
1016 <https://doi.org/10.1371/journal.pone.0303820>
1017
1018 Kaplan, J. T., Aziz-Zadeh, L., Uddin, L. Q., & Iacoboni, M. (2008). The self across the senses:
1019 an fMRI study of self-face and self-voice recognition. *Social cognitive and affective*
1020 *neuroscience*, 3(3), 218-223.
1021
1022 Keenan, J. P., Wheeler, M., Platek, S. M., Lardi, G., & Lassonde, M. (2003). Self-face
1023 processing in a callosotomy patient. *European Journal of Neuroscience*, 18(8), 2391-2395.
1024
1025 Keyser, C., & Gazzola, V. (2007). Integrating simulation and theory of mind: from self to social
1026 cognition. *Trends in cognitive sciences*, 11(5), 194-196.
1027
1028 Knoblich, G., & Flach, R. (2003). Action identity: Evidence from self-recognition, prediction, and
1029 coordination. *Consciousness and cognition*, 12(4), 620-632.
1030
1031 Kilner, J. M. (2011). More than one pathway to action understanding. *Trends in cognitive*
1032 *sciences*, 15(8), 352-357.
1033
1034 Kilteni K, Ehrsson HH (2024). Dynamic changes in somatosensory and cerebellar activity
1035 mediate temporal recalibration of self-touch. *Commun Biol.* 2024 May 3;7(1):522. doi:
1036 10.1038/s42003-024-06188-4.
1037

1038 Kilteni K, Engeler P, Boberg I, Maurex L, Ehrsson HH (2021). No evidence for somatosensory
1039 attenuation during action observation of self-touch. *Eur J Neurosci.* 2021 Oct;54(7):6422-6444.
1040 doi: 10.1111/ejn.15436.
1041
1042 Kilteni K, Andersson BJ, Houborg C, Ehrsson HH (2018). Motor imagery involves predicting the
1043 sensory consequences of the imagined movement. *Nat Commun.* 2018 Apr 24;9(1):1617. doi:
1044 10.1038/s41467-018-03989-0. PMID: 29691389; PMCID: PMC5915435.
1045
1046 Kirsch, L. P., & Cross, E. S. (2015). Additive routes to action learning: layering experience
1047 shapes engagement of the action observation network. *Cerebral Cortex*, 25(12), 4799-4811.
1048
1049 Koski, L., Iacoboni, M., Dubeau, M. C., Woods, R. P., & Mazziotta, J. C. (2003). Modulation of
1050 cortical activity during different imitative behaviors. *Journal of neurophysiology*.
1051
1052 Krachun, C., Lurz, R., Mahovetz, L. M., & Hopkins, W. D. (2019). Mirror self-recognition and its
1053 relationship to social cognition in chimpanzees. *Animal Cognition*, 22, 1171-1183.
1054
1055 Kriegeskorte, N., Mur, M., & Bandettini, P. A. (2008). Representational similarity analysis
1056 connecting the branches of systems neuroscience. *Frontiers in systems neuroscience*, 2, 4.
1057
1058 Lamm, C., Fischer, M. H., & Decety, J. (2007). Predicting the actions of others taps into one's
1059 own somatosensory representations—a functional MRI study. *Neuropsychologia*, 45(11), 2480-
1060 2491.
1061
1062 Leung, H. C., & Cai, W. (2007). Common and differential ventrolateral prefrontal activity during
1063 inhibition of hand and eye movements. *Journal of Neuroscience*, 27(37), 9893-9900.
1064
1065 Leshinskaya, A., & Caramazza, A. (2014). Nonmotor aspects of action concepts. *Journal of*
1066 *Cognitive Neuroscience*, 26(12), 2863-2879.
1067
1068 Liakakis, G., Nickel, J., & Seitz, R. (2011). Diversity of the inferior frontal gyrus—a meta-analysis
1069 of neuroimaging studies. *Behavioural brain research*, 225(1), 341-347.
1070
1071 Lieberman, M. D., Straccia, M. A., Meyer, M. L., Du, M., & Tan, K. M. (2019). Social,
1072 self,(situational), and affective processes in medial prefrontal cortex (MPFC): Causal,
1073 multivariate, and reverse inference evidence. *Neuroscience & Biobehavioral Reviews*, 99,
1074 311328.
1075
1076 Limanowski, J., & Blankenburg, F. (2016). Integration of visual and proprioceptive limb position
1077 information in human posterior parietal, premotor, and extrastriate cortex. *Journal of*
1078 *Neuroscience*, 36(9), 2582-2589.
1079
1080 Lingnau, A., & Downing, P. E. (2015). The lateral occipitotemporal cortex in action. *Trends in*
1081 *cognitive sciences*, 19(5), 268-277.
1082

1083 Lombardo, M. V., Chakrabarti, B., Bullmore, E. T., Wheelwright, S. J., Sadek, S. A., Suckling, J.,
1084 ... & Baron-Cohen, S. (2010). Shared neural circuits for mentalizing about the self and others.
1085 *Journal of cognitive neuroscience*, 22(7), 1623-1635.

1086

1087 Loula, F., Prasad, S., Harber, K., & Shiffrar, M. (2005). Recognizing people from their
1088 movement. *Journal of Experimental Psychology: Human Perception and Performance*, 31(1),
1089 210.

1090

1091 Macaluso, E., & Driver, J. (2005). Multisensory spatial interactions: a window onto functional
1092 integration in the human brain. *Trends in Neurosciences*, 28(5), 264-271.

1093

1094 Macuga, K. L., & Frey, S. H. (2011). Selective responses in right inferior frontal and
1095 supramarginal gyri differentiate between observed movements of oneself vs. another.
1096 *Neuropsychologia*, 49(5), 1202-1207.

1097

1098 McLaren, D. G., Ries, M. L., Xu, G., & Johnson, S. C. (2012). A generalized form of
1099 contextdependent psychophysiological interactions (gPPI): a comparison to standard
1100 approaches. *Neuroimage*, 61(4), 1277-1286.

1101

1102 Molnar-Szakacs, I., & Uddin, L. Q. (2013). Self-processing and the default mode network:
1103 interactions with the mirror neuron system. *Frontiers in human neuroscience*, 7, 571.

1104

1105 Morin, A., & Michaud, J. (2007). Self-awareness and the left inferior frontal gyrus: inner speech
1106 use during self-related processing. *Brain research bulletin*, 74(6), 387-396.

1107

1108 Morita, T., Tanabe, H. C., Sasaki, A. T., Shimada, K., Kakigi, R., & Sadato, N. (2014). The
1109 anterior insular and anterior cingulate cortices in emotional processing for self-face recognition.
1110 *Social cognitive and affective neuroscience*, 9(5), 570-579.

1111

1112 Muir, R. B., & Lemon, R. N. (1983). Corticospinal neurons with a special role in precision grip.
1113 *Brain research*, 261(2), 312-316.

1114

1115 Mukamel, R., Ekstrom, A. D., Kaplan, J., Iacoboni, M., & Fried, I. (2010). Single-neuron
1116 responses in humans during execution and observation of actions. *Current biology*, 20(8),
1117 750756.

1118

1119 Mumford, J., Turner, B., Ashby, G., & Poldrack, R. (2012). Deconvolving BOLD activation in
1120 event-related designs for multivoxel pattern classification analyses. *Neuroimage*, 59(3), 2636–
1121 2643. doi: 10.1016/j.neuroimage.2011.08.076

1122

1123 Nichols, T., Brett, M., Andersson, J., Wager, T., & Poline, J. B. (2005). Valid conjunction
1124 inference with the minimum statistic. *Neuroimage*, 25(3), 653-660.

1125

1126 Oosterhof, N. N., Connolly, A. C., & Haxby, J. V. (2016). CoSMoMvPA: multi-modal multivariate
1127 pattern analysis of neuroimaging data in Matlab/GNU Octave. *Frontiers in neuroinformatics*, 10,
1128 27.

1129

1130 Orgs G, Dovert A, Hagura N, Haggard P, Fink GR, Weiss PH (2016) Constructing visual
1131 perception of body movement with the motor cortex. *Cereb Cortex* 26:440–449
1132

1133 Peelen, M. V., & Downing, P. E. (2005). Selectivity for the human body in the fusiform gyrus.
1134 *Journal of neurophysiology*, 93(1), 603-608.
1135

1136 Pereira, F., & Botvinick, M. (2011). Information mapping with pattern classifiers: a comparative
1137 study. *Neuroimage*, 56(2), 476-496.
1138

1139 Pfurtscheller, G., & Neuper, C. (1997). Motor imagery activates primary sensorimotor area in
1140 humans. *Neuroscience letters*, 239(2-3), 65-68.
1141

1142 Pilgramm, S., de Haas, B., Helm, F., Zentgraf, K., Stark, R., Munzert, J., & Krüger, B. (2016).
1143 Motor imagery of hand actions: Decoding the content of motor imagery from brain activity in
1144 frontal and parietal motor areas. *Human brain mapping*, 37(1), 81-93.
1145

1146 Platek, S. M., Wathne, K., Tierney, N. G., & Thomson, J. W. (2008). Neural correlates of self-
1147 face recognition: an effect-location meta-analysis. *Brain research*, 1232, 173-184.
1148

1149 Platek, S. M., Loughhead, J. W., Gur, R. C., Busch, S., Ruparel, K., Phend, N., ... & Langleben,
1150 D. D. (2006). Neural substrates for functionally discriminating self-face from personally familiar
1151 faces. *Human brain mapping*, 27(2), 91-98.
1152

1153 Porro, C. A., Cettolo, V., Francescato, M. P., & Baraldi, P. (2000). Ipsilateral involvement of
1154 primary motor cortex during motor imagery. *European Journal of Neuroscience*, 12(8), 3059-
1155 3063.

1156 Price, C. J., & Friston, K. J. (1997). Cognitive conjunction: a new approach to brain activation
1157 experiments. *Neuroimage*, 5(4), 261-270.
1158

1159 Qin, P., & Northoff, G. (2011). How is our self related to midline regions and the default-mode
1160 network?. *Neuroimage*, 57(3), 1221-1233.
1161

1162 Qin, P., Wang, M., & Northoff, G. (2020). Linking bodily, environmental and mental states in the
1163 self—A three-level model based on a meta-analysis. *Neuroscience & biobehavioral reviews*,
1164 115, 77-95.

1165 Raine, A. (1991). The spq: A scale for the assessment of schizotypal personality based on
1166 DSMIII-r criteria. *Schizophrenia Bulletin*. <https://doi.org/10.1093/schbul/17.4.555>

- 1167 Roberts, R., Callow, N., Hardy, L., Markland, D., & Bringer, J. (2008). Movement imagery ability:
1168 development and assessment of a revised version of the vividness of movement imagery
1169 questionnaire. *Journal of Sport and Exercise Psychology*, 30(2), 200-221.
- 1170 Rissman, J., Gazzaley, A., & D'Esposito, M. (2004). Measuring functional connectivity during
1171 distinct stages of a cognitive task. *Neuroimage*, 23(2), 752-763.
- 1172 Rizzolatti, G., & Craighero, L. (2004). The mirror-neuron system. *Annu. Rev. Neurosci.*, 27,
1173 169-192.
- 1174 Rizzolatti, G., Fadiga, L., Gallese, V., & Fogassi, L. (1996). Premotor cortex and the recognition
1175 of motor actions. *Cognitive brain research*, 3(2), 131-141.
- 1176 Rizzolatti, G., Cattaneo, L., Fabbri-Destro, M., & Rozzi, S. (2014). Cortical mechanisms
1177 underlying the organization of goal-directed actions and mirror neuron-based action
1178 understanding. *Physiological reviews*, 94(2), 655-706.
- 1179 Roberts, R., Callow, N., Hardy, L., Markland, D., & Bringer, J. (2008). Movement imagery ability:
1180 Development and assessment of a revised version of the vividness of movement imagery
1181 questionnaire. *Journal of Sport and Exercise Psychology*. <https://doi.org/10.1123/jsep.30.2.200>
- 1182 Sasaki, A. T., Okamoto, Y., Kochiyama, T., Kitada, R., & Sadato, N. (2018). Distinct sensitivities
1183 of the lateral prefrontal cortex and extrastriate body area to contingency between executed and
1184 observed actions. *Cortex*, 108, 234–251.
- 1185 Saygin, A. P., & Dick, F. (2014). The emergence of mirror-like response properties from
1186 domain-general principles in vision and audition. *Behavioral and brain sciences*, 37(2), 219.
- 1187 Schmidt, Richard A. "A schema theory of discrete motor skill learning." *Psychological review*
1188 82.4 (1975): 225.
- 1189
1190 Seeley, W. W., Menon, V., Schatzberg, A. F., Keller, J., Glover, G. H., Kenna, H., ... & Greicius,
1191 M. D. (2007). Dissociable intrinsic connectivity networks for salience processing and executive
1192 control. *Journal of Neuroscience*, 27(9), 2349-2356.
- 1193 Smith, S. M., & Nichols, T. E. (2009). Threshold-free cluster enhancement: addressing problem
1194 of smoothing, threshold dependence and localisation in cluster inference. *Neuroimage*, 44(1),
1195 8398.
- 1196 Soch, J., Deserno, L., Assmann, A., Barman, A., Walter, H., Richardson-Klavehn, A., & Schott,
1197 B. H. (2017). Inhibition of information flow to the default mode network during self-reference
1198 versus reference to others. *Cerebral Cortex*, 27(8), 3930-3942.
- 1199 Sokolov AA, Zeidman P, Erb M, Rylvlin P, Friston KJ, Pavlova, MA. 2018. Structural and
1200 effective brain connectivity underlying biological motion detection. *Proc Natl Acad Sci U S A*.
1201 115:E12034–E12042.

1202
1203 Sperry, R. W., Zaidel, E., & Zaidel, D. (1979). Self recognition and social awareness in the
1204 deconnected minor hemisphere. *Neuropsychologia*, 17(2), 153-166.
1205
1206 Sperduti, M, P. Delaveau, P. Fossati, J. Nadel (2011) Different brain structures related to self-
1207 and external-agency attribution: A brief review and meta-analysis. *Brain Structure and Function*,
1208 216 (2011), pp. 151-157
1209
1210 Stetson, C., Cui, X., Montague, P. R. & Eagleman, D. M. Motor-sensory recalibration leads to an
1211 illusory reversal of action and sensation. *Neuron* 51, 651-659 (2006)
1212
1213 Sugiura, M., Kawashima, R., Nakamura, K., Okada, K., Kato, T., Nakamura, A., ... & Fukuda, H.
1214 (2000). Passive and active recognition of one's own face. *Neuroimage*, 11(1), 36-48.
1215
1216 Sugiura, M., Watanabe, J., Maeda, Y., Matsue, Y., Fukuda, H., & Kawashima, R. (2005).
1217 Cortical mechanisms of visual self-recognition. *Neuroimage*, 24(1), 143-149.
1218
1219 Sugiura, M., Sassa, Y., Jeong, H., Miura, N., Akitsuki, Y., Horie, K., ... & Kawashima, R. (2006).
1220 Multiple brain networks for visual self-recognition with different sensitivity for motion and body
1221 part. *Neuroimage*, 32(4), 1905-1917.
1222
1223 Sui, J., & Gu, X. (2017). Self as object: Emerging trends in self research. *Trends in*
1224 *neurosciences*, 40(11), 643-653.
1225
1226 Tacikowski P, Berger CC, Ehrsson HH. Dissociating the Neural Basis of Conceptual Self-
1227 Awareness from Perceptual Awareness and Unaware Self-Processing. *Cereb Cortex*. 2017 Jul
1228 1;27(7):3768-3781. doi: 10.1093/cercor/bhx004.
1229
1230 Tholen, M. G., Schurz, M., & Perner, J. (2019). The role of the IPL in person identification.
1231 *Neuropsychologia*, 129, 164-170.

1232 Turk DJ, Heatherton TF, Kelley WM, Funnell MG, Gazzaniga MS, Macrae CN (2002) Mike or
1233 me? Self-recognition in a split brain patient. *Nat Neurosci* 5:841–842

1234 Turk, D. J., Heatherton, T. F., Macrae, C. N., Kelley, W. M., & Gazzaniga, M. S. (2003). Out of
1235 contact, out of mind: the distributed nature of the self. *Annals of the New York Academy of*
1236 *Sciences*, 1001(1), 65-78.

1237 Uddin, L. Q. (2016). *Saliency network of the human brain*. Academic press.

1238 Uddin, L. Q., Kaplan, J. T., Molnar-Szakacs, I., Zaidel, E., & Iacoboni, M. (2005). Self-face
1239 recognition activates a frontoparietal “mirror” network in the right hemisphere: an event-related
1240 fMRI study. *Neuroimage*, 25(3), 926-935.
1241

1242 Uddin, L. Q., Rayman, J., & Zaidel, E. (2005). Split-brain reveals separate but equal
1243 selfrecognition in the two cerebral hemispheres. *Consciousness and cognition*, 14(3), 633-640.
1244

1245 Uddin, L. Q., Iacoboni, M., Lange, C., & Keenan, J. P. (2007). The self and social cognition: the
1246 role of cortical midline structures and mirror neurons. *Trends in cognitive sciences*, 11(4),
1247 153157.
1248

1249 Uhlmann, L., Pazen, M., van Kemenade, B. M., Steinsträter, O., Harris, L. R., Kircher, T., &
1250 Straube, B. (2020). Seeing your own or someone else's hand moving in accordance with your
1251 action: The neural interaction of agency and hand identity. *Human brain mapping*, 41(9),
1252 24742489.
1253

1254 Ürgen, B. A., Pehlivan, S., & Saygin, A. P. (2019). Distinct representations in occipito-temporal,
1255 parietal, and premotor cortex during action perception revealed by fMRI and computational
1256 modeling. *Neuropsychologia*, 127, 35-47.
1257

1258 Urgesi, C., Candidi, M., Ionta, S., & Aglioti, S. M. (2007). Representation of body identity and
1259 body actions in extrastriate body area and ventral premotor cortex. *Nature neuroscience*, 10(1),
1260 30-31.
1261

1262 van Boxtel, J. J., & Lu, H. (2013). A biological motion toolbox for reading, displaying, and
1263 manipulating motion capture data in research settings. *Journal of vision*, 13(12), 7-7.
1264

1265 Van Den Bos, E., and Jeannerod, M. (2002). Sense of body and sense of action both contribute
1266 to self-recognition. *Cognition* 85, 177–187. doi: 10.1016/S0010-0277(02)00100-2
1267

1268 van Kemenade, B. M., Arikan, B. E., Kircher, T., & Straube, B. (2017). The angular gyrus is a
1269 supramodal comparator area in action–outcome monitoring. *Brain Structure and Function*,
1270 222(8), 3691-3703.
1271

1272 Van Kemenade, B. M., Arikan, E. A., Podranski, K., Steinsträter, O., Kircher, T., & Straube, B.
1273 (2019). Distinct roles for the cerebellum, angular gyrus and middle temporal gyrus in
1274 actionfeedback monitoring. *Cerebral Cortex*, 29, 1520–1531. [https://doi.org/10.1093/cercor/
1275 bhy048](https://doi.org/10.1093/cercor/bhy048)
1276

1277 van Veluw, S. J., & Chance, S. A. (2014). Differentiating between self and others: an ALE
1278 metaanalysis of fMRI studies of self-recognition and theory of mind. *Brain imaging and behavior*,
1279 8(1), 24-38.
1280

1281 Vocks, S., Busch, M., Grönemeyer, D., Schulte, D., Herpertz, S., & Suchan, B. (2010).
1282 Differential neuronal responses to the self and others in the extrastriate body area and the
1283 fusiform body area. *Cognitive, Affective, & Behavioral Neuroscience*, 10(3), 422-429.
1284

1285 Weiner, K. S., & Grill-Spector, K. (2011). Not one extrastriate body area: using anatomical
 1286 landmarks, hMT+, and visual field maps to parcellate limb-selective activations in human lateral
 1287 occipitotemporal cortex. *Neuroimage*, 56(4), 2183-2199.

1288

1289 Winkler, A. M., Ridgway, G. R., Webster, M. A., Smith, S. M., & Nichols, T. E. (2014).
 1290 Permutation inference for the general linear model. *Neuroimage*, 92, 381-397.

1291

1292 Worsley, K. J. (2001). Statistical analysis of activation images. *Functional MRI: An introduction*
 1293 *to methods*, 14(1), 251-70.

1294

1295 Woźniak, M., Schmidt, T. T., Wu, Y. H., Blankenburg, F., & Hohwy, J. (2022). Differences in
 1296 working memory coding of biological motion attributed to oneself and others. *Human Brain*
 1297 *Mapping*.

1298

1299 Wurm, M. F., & Caramazza, A. (2021). Two 'what' pathways for action and object recognition.
 1300 *Trends in cognitive sciences*.

1301

1302 Wurm, M. F., & Lingnau, A. (2015). Decoding Actions at Different Levels of Abstraction. *Journal*
 1303 *of Neuroscience*, 35(20), 7727–7735. <https://doi.org/10.1523/JNEUROSCI.0188-15.2015>

1304

1305 Wurm, M. F., Caramazza, A., & Lingnau, A. (2017). Action categories in lateral occipitotemporal
 1306 cortex are organized along sociality and transitivity. *Journal of Neuroscience*, 37(3), 562-575.

1307

1308 Yeshurun, Y., Nguyen, M., & Hasson, U. (2021). The default mode network: where the
 1309 idiosyncratic self meets the shared social world. *Nature reviews neuroscience*, 22(3), 181-192.

1310

1311 Yovel, G., & O'Toole, A. J. (2016). Recognizing people in motion. *Trends in cognitive sciences*,
 1312 20(5), 383-395.

1313

1314

1315

1316

1317

1318 **Figure captions**

1319

1320 **Fig 1. Trial structure including timing.** Participants centrally attended to a white fixation cross
 1321 until the action (self/friend/other) appeared for 5 s. On a subsequent screen, participants were
 1322 then provided 2 s to make their identity judgment, followed by the variable ITI (mean-centered at
 1323 5 s). The response order of self, friend, other was counterbalanced in order to reduce any impact
 1324 of motor order.

1325

1326

1327 **Fig 2. Left Panel:** Representational (dis)similarity matrices (RDMs) used for each
 1328 representational dissimilarity analysis averaged across participants. RDMs reflect the Euclidean
 1329 distance between identity and action categories for speed, movement distinctiveness and body

1330 structure. For motor familiarity, identity was based on the degree of motor dissimilarity to oneself
1331 (self-generated actions, i.e., verbal instruction: zero dissimilarity; self-imitated actions, i.e., visual
1332 instruction: small dissimilarity, 0.3; friend actions: medium dissimilarity, 0.6; strangers: most
1333 dissimilarity, 1). Brighter colors for all RDMs indicate more dissimilarity. *Top Right Panel:* Upper
1334 triangular pairwise dissimilarity (1 – spearman’s rho) between each of the group-level RDMs.
1335 Brighter colors indicate more dissimilarity. *Bottom Right Panel:* DTW figure showing movement
1336 trajectory of one joint from one actor’s action time series (shown as red dots indicating locations)
1337 with lines measuring similarity to the corresponding joint in another actor’s time series (shown as
1338 green dots) to find the optimal decrease in dissimilarity over time.

1339
1340 **Fig 3. Behavioral results of identity recognition accuracy.** *Top:* Self-recognition performance
1341 for different actions color coded by action type (verbal instruction: gray; visual instruction: blue).
1342 Light gray fill indicates bar plots for verbal instruction. Light blue fill indicates bar plot for visual
1343 instruction. Inference bands denote 95% Bayesian highest density interval with 1000 iterations.
1344 Horizontal blue line indicates chance-level recognition accuracy (.33). *Bottom left panel:* depicts
1345 confusion matrix for each identity. No significant misattributions were found for the self relative
1346 to other identities, though friend and stranger were more confused relative to the self (~55%
1347 increase in misattributions for friend and strangers). *Bottom right panel:* average recognition
1348 accuracy for each identity. All identities were recognized significantly above chance. Self actions
1349 were recognized significantly better than friend actions. Light gray fill indicates bar plots.
1350 Inference bands denote 95% Bayesian highest density interval with 1000 iterations. Horizontal
1351 blue line indicates chance-level recognition accuracy (.33). * $p < .05$, ** $p < .01$, *** $p < .001$.

1352
1353

1354 **Fig 4.** Group-level activity obtained using FSL’s non-parametric permutation approach
1355 (*randomise*) with TFCE, $p < .05$. *From Left to Right:* Self v baseline; friend v baseline; and
1356 stranger v baseline.

1357 † Large cluster sizes were obtained with TFCE due to the optimal cluster-defining threshold;
1358 hence cluster peaks are reported with visual interpolation using manual thresholding with a
1359 sliding scale. *Abbreviations:* Inferior Frontal Cortex (IFC); Superior Temporal Sulcus (STS);
1360 Lateral Occipital Cortex (LOC); Supplementary Motor Area (SMA); Supramarginal Gyrus (SMG);
1361 Angular Gyrus (Ang).

1362
1363 **Fig 5. Univariate group-level activity for self > stranger (left) and self > friend (right) using**
1364 **the FSL *randomise* permutation approach**, cluster corrected with TFCE ($p < .05$). Violin plot
1365 shows mean parameter estimates (PE) for the left posterior supramarginal gyrus (SMG) for all
1366 identities. The left SMG significantly discriminated contrasts of PE for both self vs stranger ($p =$
1367 $.001$) and self vs friend ($p = .005$), but not friend vs stranger ($p = .821$). Extended Data Figures
1368 5-1 and 5-3 report the activity maps and peak clusters for both TFCE contrasts, as well as RFT
1369 cluster-corrected results (Figures 5-2 and 5-5).

1370

1371 **Fig 6. Task-modulated functional connectivity of left and right IPL.** Left IPL (top panel)
1372 seed showed increased connectivity with bilateral occipito-temporal regions, bilateral superior
1373 and inferior parietal areas, and bilateral inferior frontal cortex during *self > stranger*. For *self >*
1374 *friend*, functional connectivity analysis revealed greater connectivity with the bilateral inferior
1375 frontal cortices and occipito-temporal regions. Task-modulated functional connectivity of the
1376 right IPL (bottom panel) showed a similar activity pattern to the left: strengthened fronto-parietal
1377 and parieto-occipital connectivity for both contrasts. All activity cluster corrected at $Z > 2.3$, $p <$
1378 $.01$. Abbreviations: IPL (Inferior Parietal Lobule), IPS (Intraparietal Sulcus), IFC (Inferior Frontal
1379 Cortex), OT (Occipito-Temporal Regions), EBA (Extrastriate Body Area), STS (Superior
1380 Temporal Sulcus).

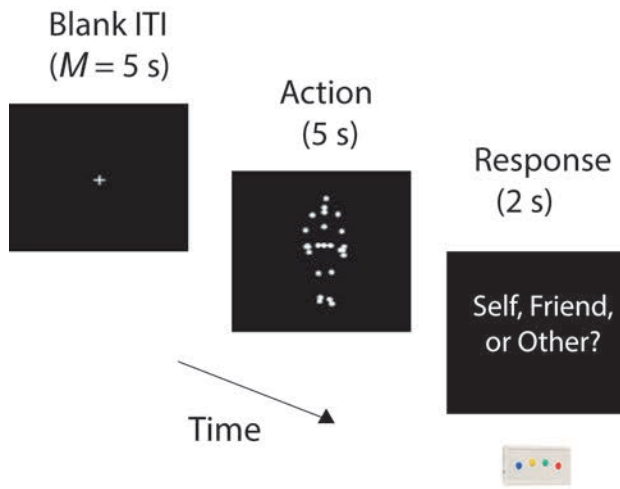
1381
1382 **Fig 7. Multiple regression searchlight RDA results for motor familiarity.** This figure
1383 depicts the z-transformed activity map for significant correlations between the motor
1384 familiarity RDM and the neural RDM based on activity patterns for actions (self encoded as
1385 least dissimilar, with action separation to account for motor familiarity between action types;
1386 friend as medium dissimilarity, stranger as most), after accounting for speed and movement
1387 distinctiveness (DTW). Activation map reflects brain activity after 10000 non-parametric
1388 Monte Carlo simulations, using TFCE and $p < 0.01$. *Regions*: bilateral somato-motor cortex:
1389 primary motor cortex, primary somatosensory cortex, superior parietal lobule; frontoparietal
1390 cortex: inferior parietal lobule, inferior frontal cortex, medial prefrontal cortex; occipito-
1391 temporal cortex: inferior temporal cortex, superior temporal sulcus and gyrus. All activity
1392 patterns are reported in Extended Data Table 7-1.

1393 **Fig 8. Multiple regression searchlight RDA results for each identity (self, friend, stranger).**
1394 Activation maps reflect TFCE-corrected brain activity after 10000 non-parametric Monte Carlo
1395 simulations, $p < 0.01$ for self and friend; $p < .05$ for stranger. Dissimilarity matrices reflect
1396 dissimilarity based on identity across all actions. *Regions*: Frontoparietal: Inferior Parietal lobule;
1397 Superior Frontal Gyrus, lateral and medial prefrontal cortices. Somatomotor: Primary Motor
1398 Cortex (M1), Primary Somatosensory Cortex (S1). Occipito-Temporal: Superior Temporal
1399 Sulcus, Middle Temporal Gyrus, Extrastriate Body Area. Activity patterns are reported in
1400 Extended Data Tables 8-1, 8-2, 8-3, 8-4 and Figure 8-1.

1401
1402 **Fig 9. Multiple regression searchlight RDA results for self identity, regressing out motor**
1403 **responses.** Activation maps reflect TFCE-corrected brain activity after 10000 non-parametric
1404 Monte Carlo simulations, $p < 0.01$ for self. Dissimilarity matrix reflects dissimilarity based on self-
1405 identity across all actions. *Regions*: Frontoparietal: Inferior Parietal lobule; Superior Frontal
1406 Gyrus, lateral and medial prefrontal cortices. Somatomotor: Primary Motor Cortex (M1), Primary
1407 Somatosensory Cortex (S1). Occipito-Temporal: Superior Temporal Sulcus, Middle Temporal
1408 Gyrus, Extrastriate Body Area. Activity patterns are reported in Extended Data Table 9-1.

1409

1410

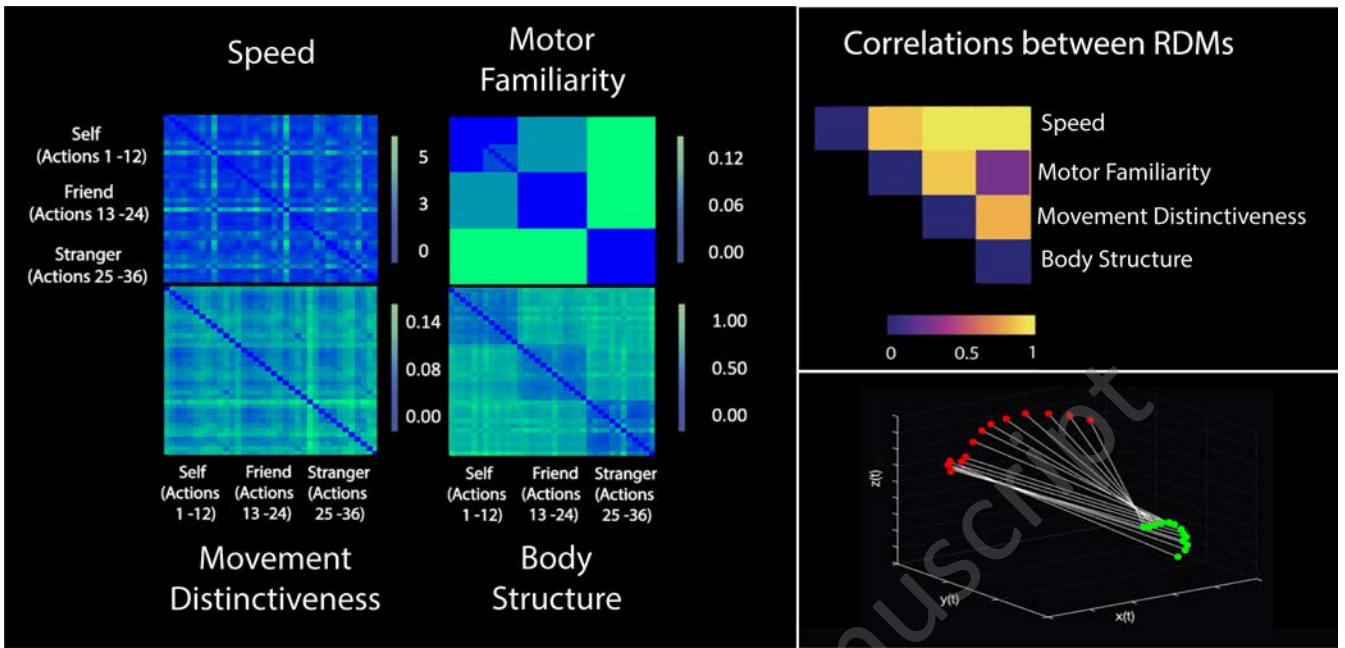


Action Types

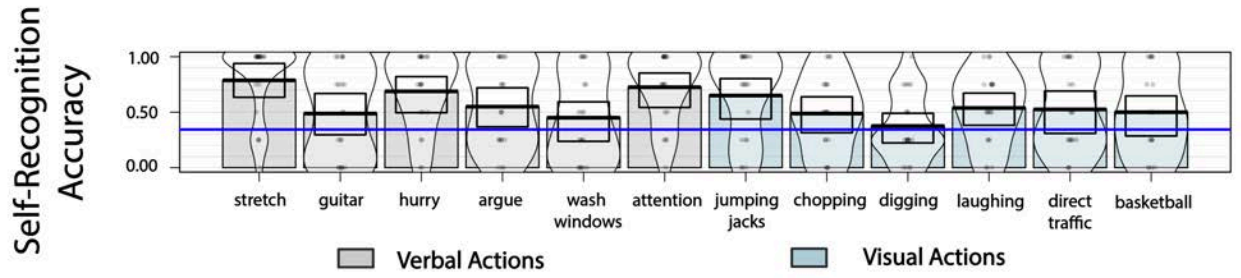
Verbal Instruction (6): Stretch, Guitar, Hurry Up, Get Attention, Wash Windows

Visual Instruction (6): Jumping Jacks, Direct Traffic, Laughing, Basketball, Chopping, Digging

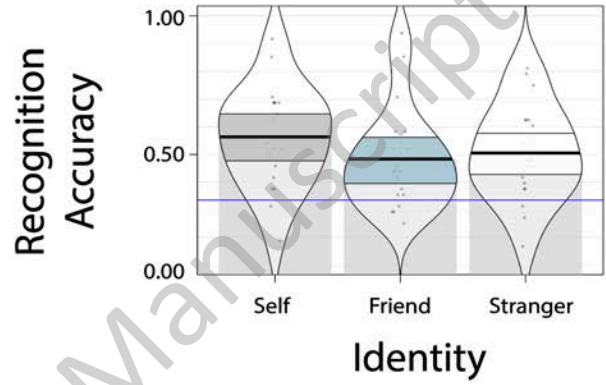
JNeurosci Accepted Manuscript



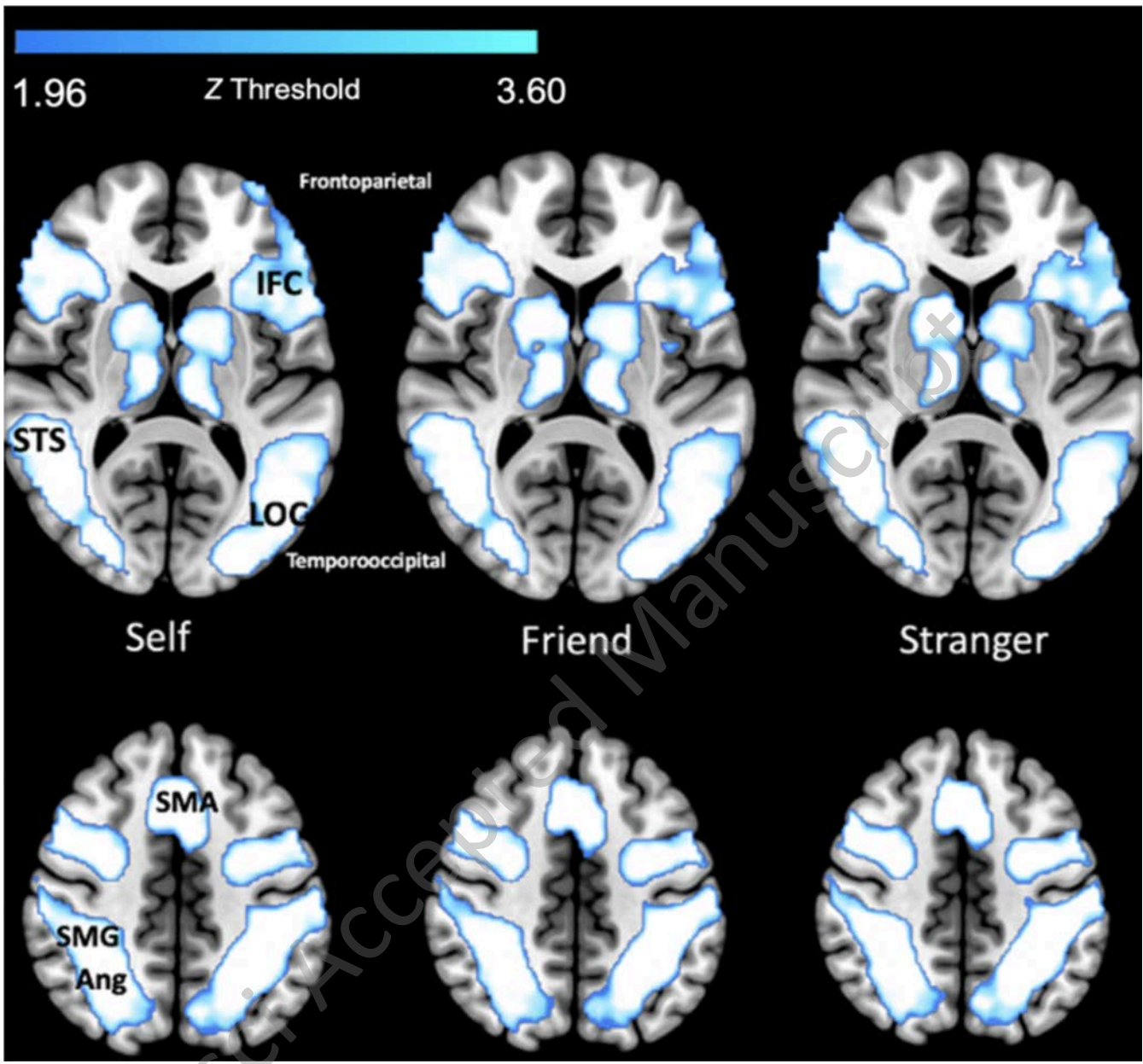
JNeurosci Accepted Manuscript



True Class	Predicted Class		
	Self	Friend	Stranger
Self	56.8%	18.5%	24.8%
Friend	16.4%	48.6%	35.0%
Stranger	16.6%	32.3%	51.2%

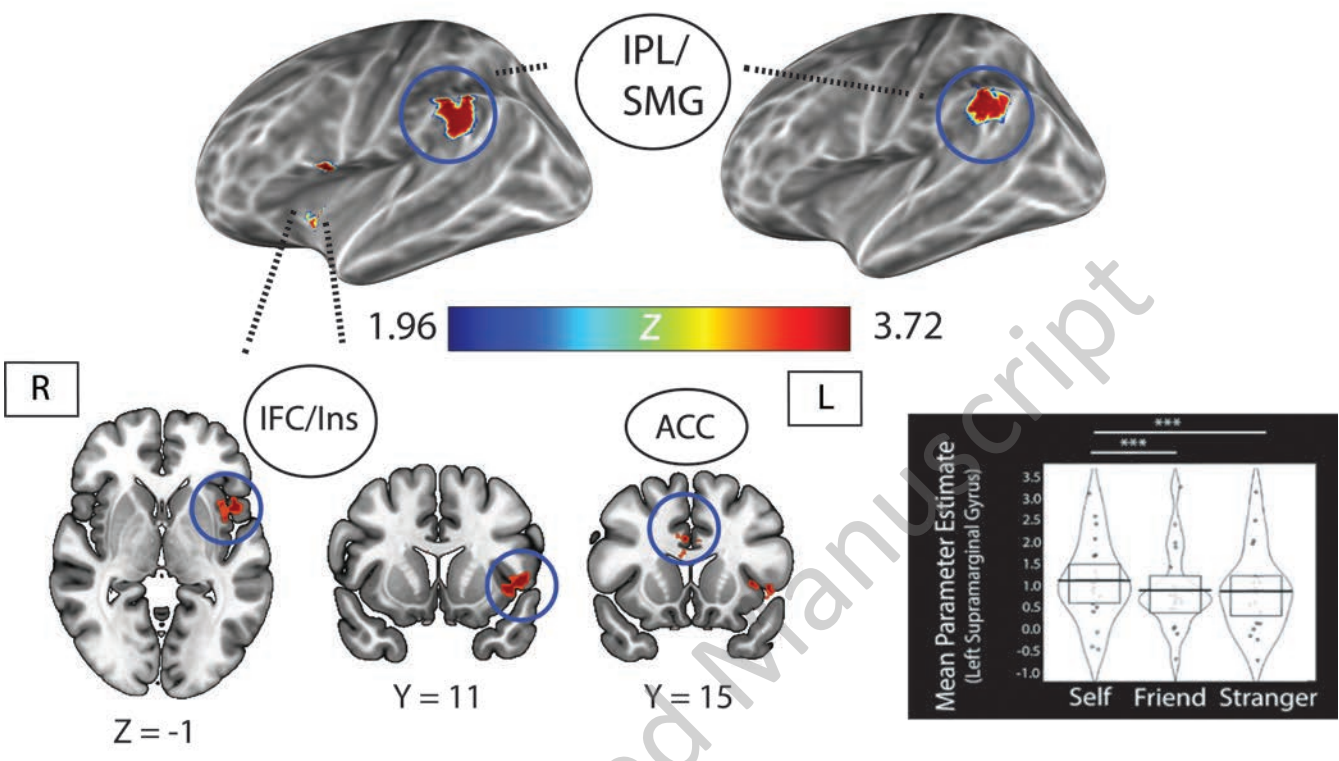


JNeurosci Accepted Manuscript



L Self > Stranger

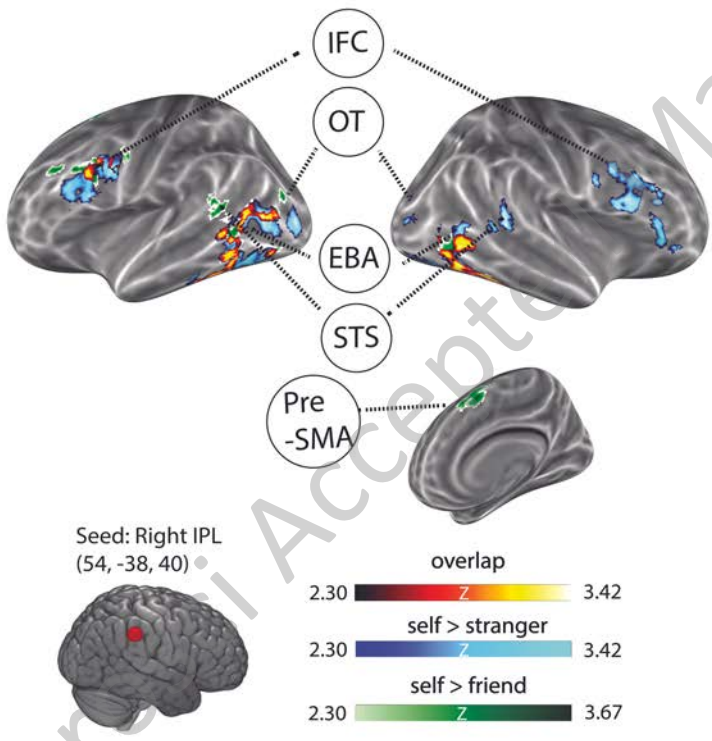
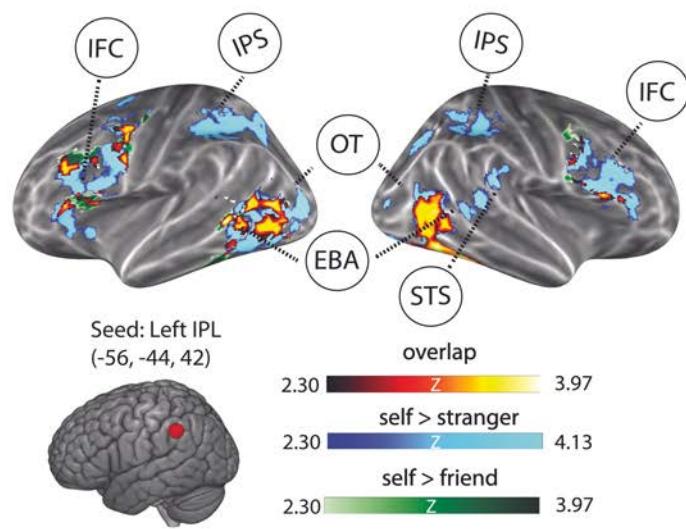
L Self > Friend



JNeurosci Accepted Manuscript

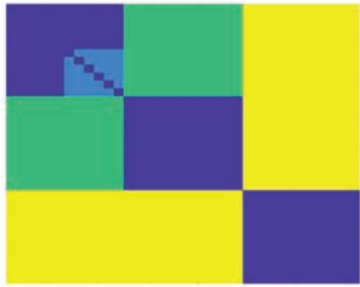
L

R

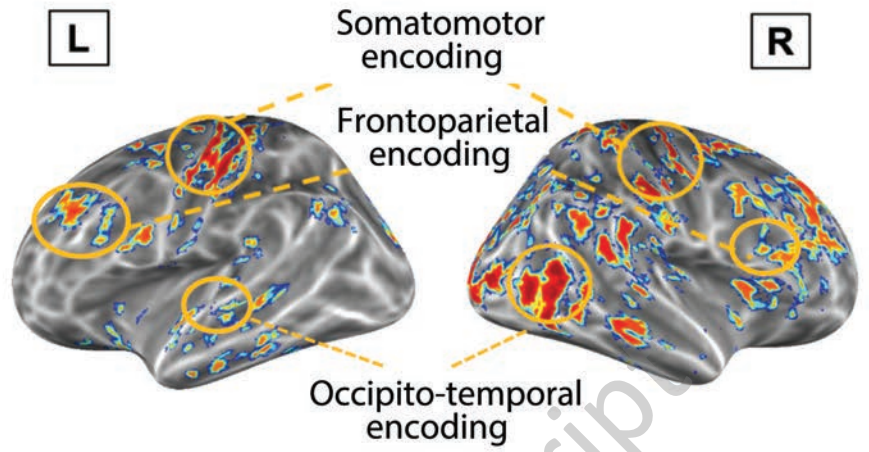


JNeurosci Accepted Manuscript

Motor Familiarity



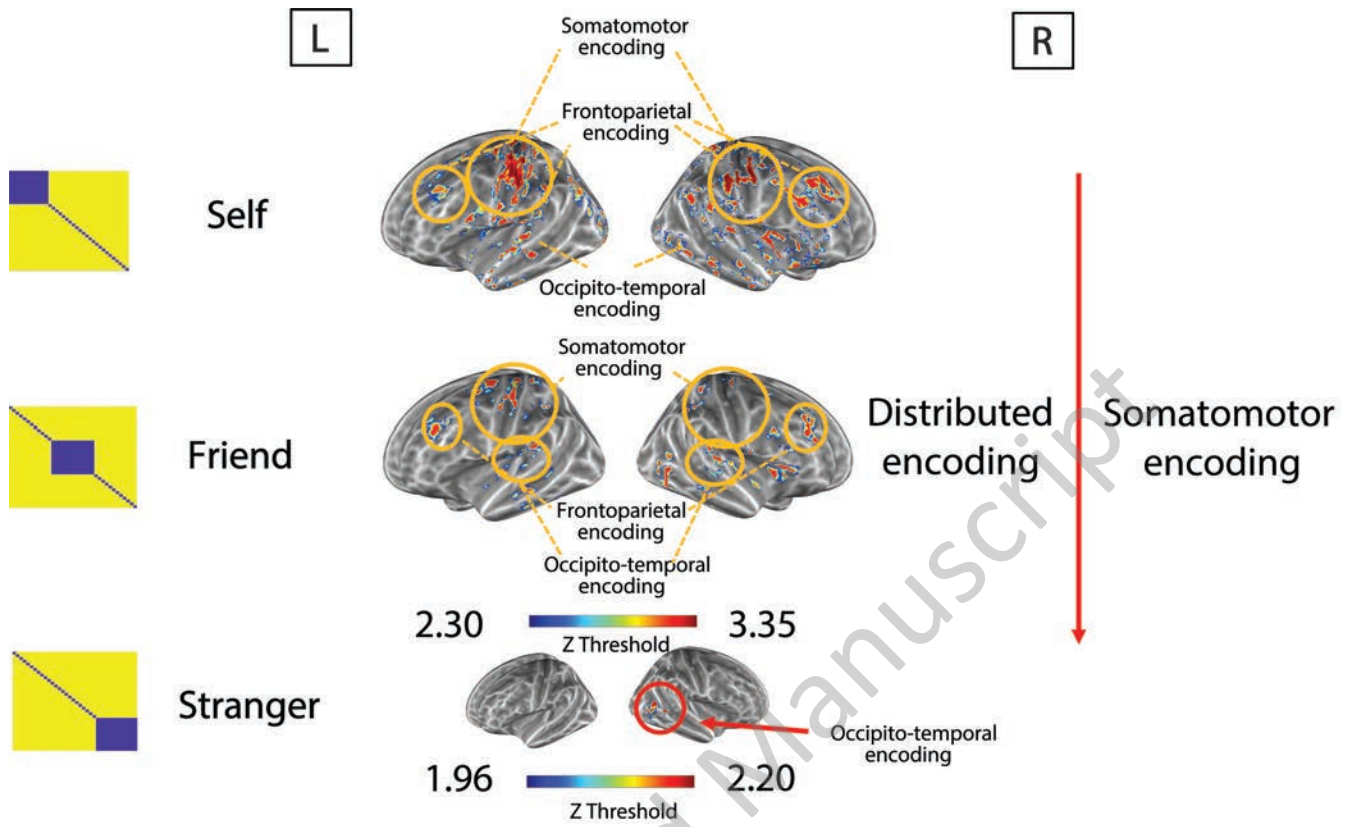
L



R



JNeurosci Accepted Manuscript



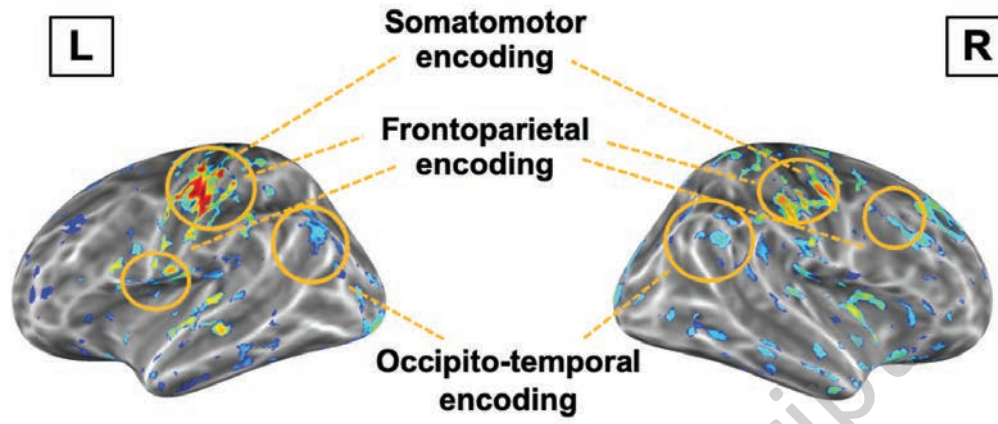
JNeurosci Accepted Manuscript



Self

L

R



JNeurosci Accepted Manuscript